Politecnico di Torino

Avio Aero
a GE Aerospace company

Department of Mechanical and Aerospace Engineering
Master' s Degree in
AEROSPACE ENGINEERING

Master' s Degree THESIS

DEVELOPMENT OF A ROTOR BALANCING TOOL FOR AERONAUTICAL ENGINE APPLICATION

Supervisor:
Prof. Christian Maria FIRRONE
Company Tutor:
Matteo FURFARO

Candidate:
Matteo TROVATO

October 2023

Abstract

Rotor's unbalance is a synchronous dynamic load which is source of vibrations, especially on Aircraft engines. These vibrations could lead to hardware failure because of High Cycle Fatigue and it could impact the overall performance of the machine, with even the possibility of a catastrophic event in case the rotor operates at one of its critical speeds. The main goal of rotordynamic analysis is to study the effects of rotor unbalance, predicting and optimizing the modal response of the machine and verifying it through measurements of the resulting vibrations. Residual unbalance is intrinsic of any rotor assembly process and cannot be completely removed. In order to reduce the vibration response, the residual unbalance should be minimized through a dedicated balancing process.

This thesis work, done in association with Avio Aero, is focused on the study of the balancing process, with the final goal of developing a tool that is able to perform all the necessary steps. Starting from available field test performed on a turboprop engine, measured vibrations from different trial configurations are analyzed and processed to find how the engine react to a certain weight change. These data are then elaborated by the tool in order to find the best balance solution for the propeller, which is one of the main sources of unbalance in the turboprop engine applications.

To my Family

Acknowledgements

I would like to express my gratitude to my tutor Matteo Furfaro and my supervisor prof. Christian Maria Firrone, for their guidance and their help during these last months.

I am grateful to my family, especially to my parents and my grandparents, who raised me and supported me with love, and made me the person I am now. And to my brother, who is always there when I need him, no matter how annoying he can be.

And last but not least, I want to thank all of my friends, old and new, for they are the ones who keep me sane in this crazy world, and who always make me laugh and cheer me up when I need it the most.

All these people are the lights that brighten up my path and I will always cherish every single moment lived together. This is the way.

Table of Contents

List of Tables VII

List of Figures VIII

1 Introduction 1

2 Fundamentals of Rotordynamics 3

2.1 Linear model 3

2.2 Complex coordinates 5

2.3 Free vibration and Campbell diagrams 6

2.4 Forced response 11

3 Rotordynamics modeling and analysis 13

3.1 Spring-mass model 14

3.1.1 Undamped system 14

3.2 Jeffcott rotor 15

3.3 Beam model and 2D analysis 20

4 Test data analysis 23

4.1 Signal analysis 23

4.1.1 Accelerometers 24

4.1.2 Keyphasor 27

4.2 Response vector calculation 28

4.2.1 Filtered signal 29

4.2.2 Phase calculation 31

4.2.3 Amplitude calculation 36

4.2.4 Output of the analysis 38

4.2.5 Other response analysis features 40

5 Balancing through sensitivity coefficient 42

5.1 Sensitivity factor 43

5.1.1 Single plane 45

5.1.2 Two-planes balancing 47

5.2 Best balance solution 52

6 Testing and validation of the tool 56

6.1 Two planes balancing 56

6.2 Trim balancing 61

6.3 Validation through test data 63

6.4 Effect of the bandwidth on the 1/rev response 65

7 Conclusion 71

Bibliography 73

List of Tables

6.1 Weights applied on the different test runs 64

List of Figures

2.1 Example of phasor in vector and sinusoidal form [10] 7

2.2 Campbell diagram represented on the first quadrant [4] . . . 8

2.3 Campbell diagram with separated forward and backward whirling and synchronous forcing function [4] 10

2.4 Campbell diagram with different engine orders responses [12] 12

3.1 Single degree of freedom spring-mass model [13] 15

3.2 Jeffcott rotor at rest (a) and in displaced configuration (b) . 16

3.3 End view of a whirling rotor in displaced position 17

3.4 Imbalance response: amplitude (a) and phase (b) [5] 19

3.5 Example of a simple rotor seen as a beam model 22

4.1 Piezoelectric accelerometer [8] 24

4.2 ENDEVCO 2221F piezoelectric accelerometer [11] 25

4.3 Circumferential position of the accelerometers with reference AFT Looking Forward 26

4.4 Example of vibrations measured by the accelerometers . . . 26

4.5 Keyphasor giving a once per turn signal to measure the blade speed and position 27
4.6 Keyphasor signal 28
4.7 Keyphasor signal preview box 29
4.8 Band pass filter Bode plot 30
4.9 1/rev filtered response signal 32
4.10 Analysis parameters selection window 32
4.11 Visualization of phase lag convention 33
4.12 Phase discontinuity (a) and corresponding signal (b) 35
4.13 Same phase from figure 4.12a shown in continuous form . . . 36
4.14 Block division (a) with corresponding RMS (b) 37
4.15 Response amplitude (a) and phase (b) plotted as output . . 39
4.16 Sensitivity factor calculation window with buttons to interact with response files 40
4.17 Response file creation panel 41

5.1 Unbalance vector Wt 43
5.2 Graphical representation of a balancing vector solution [6] . 44
5.3 Baseline (a) and trial (b) rotor configurations 45
5.4 Baseline (a), trial 1 (b) and trial 2 (c) rotor configurations for the ideal case 49
5.5 Baseline (a), trial 1 (b) and trial 2 (c) rotor configurations for the general case 50
5.6 Tool interface with solution displayed 55

6.1 Rotor model used for 2D analysis 56
6.2 Displaced rotor corresponding to mode 1 (a) mode 2 (b) and mode 3 (c) 57
6.3 Baseline response of mode 1 rotor (a) with the responses resulting from balancing respectively with s_1 (b), s_2 (c) and s_3 (d) 58
6.4 Baseline response of mode 2 rotor (a) with the responses resulting from balancing respectively with s_1 (b), s_2 (c) and s_3 (d) 59
6.5 Baseline response of mode 3 rotor (a) with the responses resulting from balancing respectively with s_1 (b), s_2 (c) and s_3 (d) 60
6.6 Response of mode 3 rotor after balancing at its critical speed 61
6.7 Baseline response of mode 1 rotor (a) with the responses resulting from balancing (b) 62
6.8 Baseline response of mode 2 rotor (a) with the responses resulting from balancing (b) 63
6.9 Baseline response of mode 3 rotor (a) with the responses resulting from balancing (b) 63
6.10 Balance solutions from tool for combination 1 (a), 2 (b) and 3 (c) 65
6.11 Error message displayed in case of 1/rev with wrong frequency 66
6.12 1/rev responses obtained with different filter bandwidths . . 67
6.13 1/rev response signal with and without noise 68
6.14 Frequency domain response in a point without noise on the 1/rev 69

6.15 Frequency domain response in a point with noise on the 1/rev 70

Chapter 1

Introduction

Rotors are one of the most commonly used components of machines and mechanisms. A rotor is defined as a body that rotates freely about an axis, usually with a significant angular momentum. If the spin axis is not in a fixed position in space, the body can be defined as a *free rotor*. In a machine, however, the rotor is suspended by bearings or hinges in a way that locks the axis position in space. This type of rotor is called *fixed rotor*. The non-rotating parts of the machine are usually defined as stator.

Rotors are a fundamental part of the most used aeronautical engine architectures. Compressors, turbines and propellers are all defined as rotors. Because of this and their operating speed, rotors are the main source of perturbations in an aeronautical engine. The rotational motion is used to convert kinds of energy, like the thermal energy from the combustion, into kinetic energy. This energy cannot be fully converted in the intended way, part of it is dissipated, for example, as thermal energy.
In rotors other kinds of energy leak occurs, converting rotational energy in other forms of mechanical energy. These side effects can cause vibrations in the rotors, that are transferred to the stator parts of the machine through

the supporting bearing and the fluid around the rotor. Given the high rotational speeds involved, these vibrations can be more and more pronounced, becoming particularly dangerous for the integrity of the structure. Rotor vibrations have three main modes: lateral, torsional and axial mode. The one that brings more concern between the three is the lateral mode.
One of the principal causes of these perturbations is the inevitable unbalance present in a practical rotor, which produces a rotating force vector and a consequent rotating displacement vector, resulting in vibrations of the machinery in the aforementioned lateral mode, which can be called synchronous vibrations.[8, 4]

One goal of rotodynamic analysis is to study the effects of rotor unbalance, predicting critical speeds and natural frequencies, in order to optimize the modal response of the system. This optimization is done through a balancing process that aims to reduce as much as possible the residual unbalance.
The main focus of the present paper will be the development of a tool based on an already existing working tool, GE's Multibal, that allows to perform the entire balancing process. The new tool developed takes the balance solution calculation from the previous one, and adds the preliminary analysis and processing of raw field data test, necessary to find the responses to unbalance of the rotor. These responses are measured for the same rotor under different unbalance configuration and are compared to find how a certain mass change acts on the vibration and to end with an optimized balance solution. This solution is given in the form of a balancing mass and its ideal position.
The objective is then to improve the already existing tool, allowing to further automatize the entire process and adding a more user friendly visual interface.

Chapter 2

Fundamentals of Rotordynamics

2.1 Linear model

The equations that describe even the simplest rotor are fairly complex and do not allow the direct use of a linear model. Therefore, a number of assumptions are made in order to obtain a linearized model which can describe correctly the behavior of a rotating system, both qualitatively and quantitatively. These assumptions are those of small displacements and velocities, with the unbalance considered as a small perturbation.
The rotation about the spin axis, which cannot be considered small, is instead considered as constant or as imposed by the driving system. Under these conditions the rotor is axially symmetrical, with a rotation axis corresponding to one of the barycentric principal axes of inertia.
These assumptions allow to obtain the linearized equation of motion in the general form:

$$\mathbf{M}\ddot{\mathbf{q}}(t) + (\mathbf{C} + \mathbf{G})\dot{\mathbf{q}}(t) + (\mathbf{K} + \mathbf{H})\mathbf{q}(t) = \mathbf{f}(t) \tag{2.1}$$

- $\mathbf{q}$(t) = generalized coordinates vector.
- $\mathbf{M}$ = symmetric mass matrix.
- $\mathbf{C}$ = symmetric damping matrix.
- $\mathbf{G}$ = skew-symmetric gyroscopic matrix.
- $\mathbf{K}$ = symmetric stiffness matrix.
- $\mathbf{H}$ = skew-symmetric circulatory matrix.
- $\mathbf{f}$(t) = time dependent vector of forcing functions.

As seen before, one of the main forcing functions is the rotor unbalance. These forces are harmonic functions with frequency equal to the rotational speed Ω and amplitude proportional to Ω^2.
The matrix $\mathbf{G}$ contains inertial terms that are linked to the gyroscopic moments acting on the rotating components. In case of reference to a non-inertial frame, there are also terms associated to Coriolis acceleration included. Matrix $\mathbf{H}$ includes terms given by the internal damping of the rotor, and in case of a linearized model for fluid bearings, also by the damping of the fluid film around it. These two matrices are proportional to the speed Ω and reduce the equation to that of a still structure when this value tends to zero.
Matrices $\mathbf{C}$ and $\mathbf{K}$ can also be dependent on the spin speed, usually on its square Ω^2. [4]

2.2 Complex coordinates

When stator and rotor are both isotropic with respect to the rotation axis, it is possible to simplify the equation of motion by introducing complex coordinates.[4]
Considering a rotor with spin axis coincident with the z-axis of an inertial frame, the lateral displacement can be described in terms of a displacement vector in the xy-plane in the form of a complex number

$$r(t) = x(t) + iy(t), \tag{2.2}$$

with $i = \sqrt{-1}$ imaginary unit. This is in a way equivalent to define the displacement vector as

$$r(t) = \begin{Bmatrix} x(t) \\ y(t) \end{Bmatrix}. \tag{2.3}$$

When using complex coordinates, the equation of motion can be written as

$$\mathbf{M}'\ddot{\mathbf{q}}'(t) + (\mathbf{C}' + i\mathbf{G}')\dot{\mathbf{q}}'(t) + (\mathbf{K}' + i\mathbf{H}')\mathbf{q}'(t) = \mathbf{f}'(t), \tag{2.4}$$

that, substituting the expression of $\mathbf{q}'(t)$ and separating the real and imaginary components

$$\mathbf{q}(t) = \begin{Bmatrix} Re(\mathbf{q}'(t)) \\ Im(\mathbf{q}'(t)) \end{Bmatrix}, \tag{2.5}$$

becomes

$$\begin{bmatrix} \mathbf{M}' & 0 \\ 0 & \mathbf{M}' \end{bmatrix} \ddot{\mathbf{q}}(t) + \left(\begin{bmatrix} \mathbf{C}' & 0 \\ 0 & \mathbf{C}' \end{bmatrix} + \begin{bmatrix} 0 & -\mathbf{G}' \\ \mathbf{G}' & 0 \end{bmatrix} \right) \dot{\mathbf{q}}(t) + \\ + \left(\begin{bmatrix} \mathbf{K}' & 0 \\ 0 & \mathbf{K}' \end{bmatrix} + \begin{bmatrix} 0 & -\mathbf{H}' \\ \mathbf{H}' & 0 \end{bmatrix} \right) \mathbf{q}(t) = \mathbf{f}(t). \tag{2.6}$$

When written in this form, the matrices that where previously symmetric are now real, while the ones that were skew-symmetric become symmetric, imaginary terms. This way all relevant matrices are then symmetric.
In this paper, the complex coordinates are treated as phasors, allowing different ways to represent the same information. A phasor is a complex number that describes a sinusoidal function with amplitude ad initial phase that are constant with time.
Writing the displacements and unbalance vectors as complex numbers can be seen as using cartesian coordinates, as seen in equation 2.3. This will be useful in this work when performing the calculations needed to balance the rotors. When given with the purpose of displaying them as output data to be interpreted by the reader, however, these vectors will instead be written in polar coordinates as amplitude and phase, which is a more intuitive format to visualize. The use of phasors also allows an easy conversion of harmonic responses measured in a rotor into complex coordinates.

2.3 Free vibration and Campbell diagrams

The free behavior of the system can be found by introducing the *complex frequency* $s = \sigma + i\omega$, allowing the solution to be written in the form

$$\mathbf{q}(t) = \mathbf{q}_0 e^{st}. \tag{2.7}$$

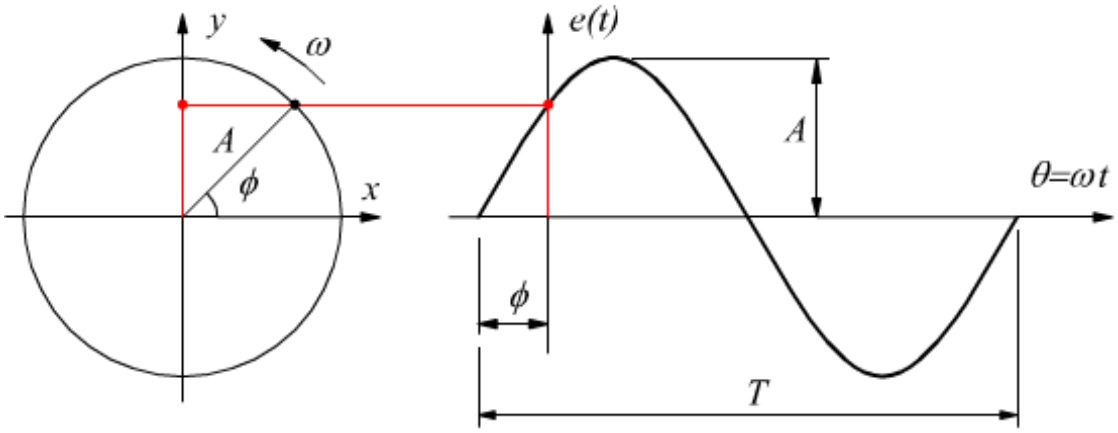

Figure 2.1: Example of phasor in vector and sinusoidal form [10]

The imaginary part ω of s is called *whirl frequency* and represents the natural frequency of the free motion, while the real part σ is the *decay rate* changed in sign. A negative value σ indicates a stable motion that decays in time, while a positive value represents an unstable motion, which grows exponentially in time.

Since both the natural frequencies and the frequencies of the exciting forces in a system can depend on the spin speed, its behavior is usually summarized through the *Campbell diagram*, which is a plot of said natural frequencies ω as functions of Ω. The diagram is symmetrical with respect to both axis, as the direction of rotation has no influence on the natural frequencies. This allows to consider only one of its quadrants, which presents all needed information.

The intersection of the diagram with the ω are the natural frequencies at standstill. From each of these points usually can stem two branches that diverge with the increasing spin speed. These can be seen as the frequencies of two different circular whirling motions, one in the same direction of the spin called *forward whirling* and one in the opposite direction called *backward*

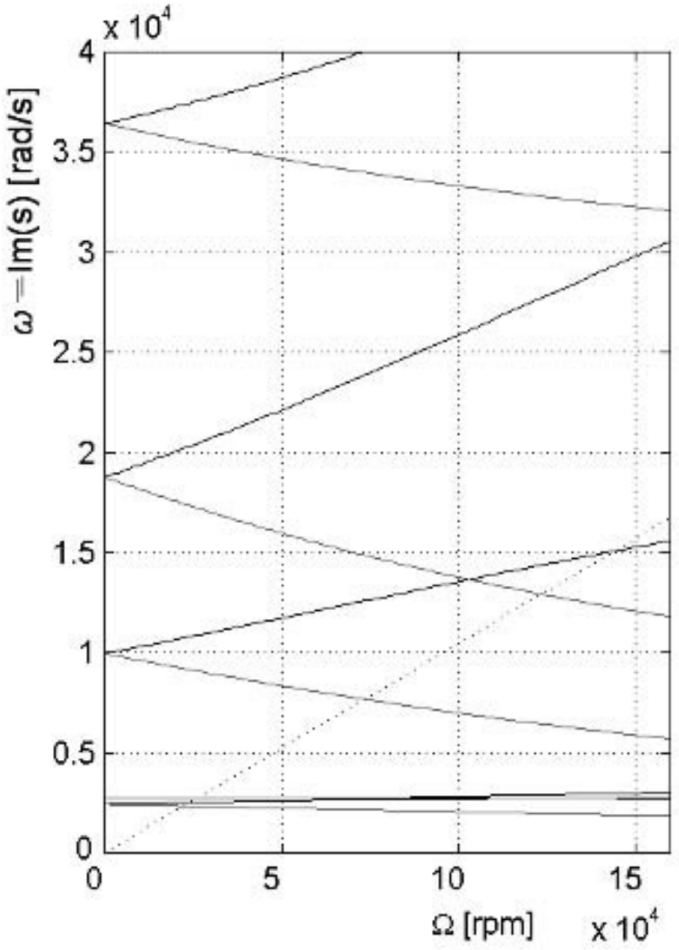

Figure 2.2: Campbell diagram represented on the first quadrant [4]

whirling. It is then possible to plot the diagram in a more clear way, using two quadrants to differentiate the two whirling motions, with positive values of ω for forward whirling and negative values for backward whirling.

External forces effecting a rotor are often variable in time, and if their time history is periodic they can always be represented as harmonics or a sum of harmonics. When this occurs, the frequency of the forcing function is often linked to the spin speed and can be plotted on the Campbell diagram. The relationship linking them is often of simple proportionality, so the forcing

function can be represented as a straight line through the origin. The forcing function given by unbalance can be seen as a vector rotating at the same speed of the rotor, resulting in the line corresponding to $\omega = \Omega$, which is the bisector of the first quadrant.
The intersection of the forcing function curves with the natural frequency curves identifies the spin speeds at which the frequency of one of the forcing coincides with one of the natural frequencies. These spin speeds are called *critical speeds*. Not all these speed are equally dangerous. In case of an intersection between the curves relating to a forcing function and a mode that are completely uncoupled form each other no resonance actually occurs.

A particularly dangerous case are the *flexural critical speeds*, that are given by the coincidence of a flexural natural frequency with the spin speed. This case correspond to the intersection of the natural frequency with the straight line $\omega = \Omega$, which happens in the presence of a synchronous excitation such as the rotor unbalance.
When an axi-symmetrical system is operating at a flexural critical speed, a circular synchronous whirling occurs. With the whirl speed equal to the spin speed the rotor is rotating in a bent configuration, with a portion of the cross section that is under a constant tensile stress and the other portion under a constant compression.
In this configuration the rotor is not vibrating, but it is a source of strong vibrations in the non rotating parts of the system, with amplitude that grows linearly in time. Since the rotor is not vibrating, the internal damping of its material is not effective in dissipating the energy, leaving only the the dumping of the stator and the supports to prevent the failure of the machine. An appropriate balancing of the rotor is then necessary to make sure that these dangerous critical speeds are not present in the operational range of the machine.

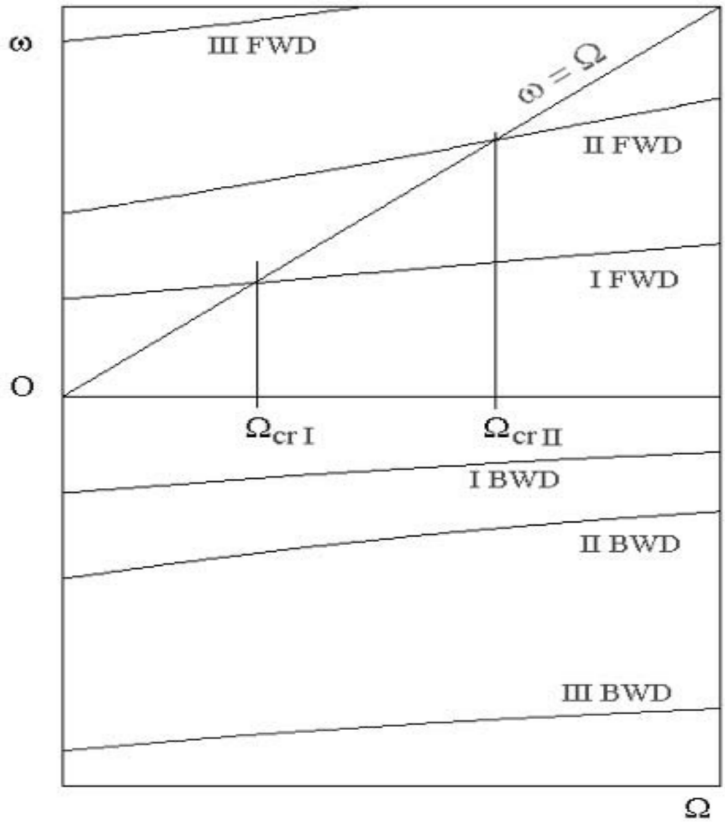

Figure 2.3: Campbell diagram with separated forward and backward whirling and synchronous forcing function [4]

It is important to note that the definition of critical speed seen above is valid only in case of a linear system. A more general definition can be used with nonlinear rotors, considering the critical speeds as the spin speeds at which the maximum amplitude of vibration is reached. With this definition the critical speeds depend also on the strength of the forcing function, while the critical speeds of linear systems are characteristic of the system and do not depend from the exciting force.

2.4 Forced response

The analysis of vibrations generated as a response to the forcing functions allows to obtain useful information on the working conditions of the machine and to predict possible problems in order to prevent them. Generally speaking, vibrations in an aeronautical engine are an unwanted side effect, so that the goal of the analysis is to minimize them as much as possible, or at least make sure that the vibration peaks do not fall into the operational speed range.

The work in this paper will focus on the effects of unbalance on rotors, but that is not the only forcing function acting on a rotating system. The synchronous component is always present, and often the most relevant one, but it is usually followed by other components. This makes the measured response not an harmonic vibration, but more a polyharmonic one that is the sum of the different harmonic responses combined together. The synchronous component is often called the *1/rev* component, while those that have frequencies multiples of the spin speed are the 2/rev, 3/rev, 4/rev, etc. components, also called *engine orders*. In order to study the response to unbalance it is then necessary to isolate the 1/rev component of the vibration.

As already seen before, in an axial symmetric system the response to unbalance is a circular whirl at the same speed Ω of the rotor. Under these conditions the rotor is spinning in a deflected configuration without vibrations, nullifying the effects of the internal damping of the material. In un undamped system this phenomenon causes vibrations on the static parts of the machine, whose amplitude goes to infinity in correspondence of the critical speed. In real machines is not possible to have an infinite value of amplitude, since they are always inherently damped, so a vibration peak is obtained at the critical speed instead. To reduce these peaks its necessary

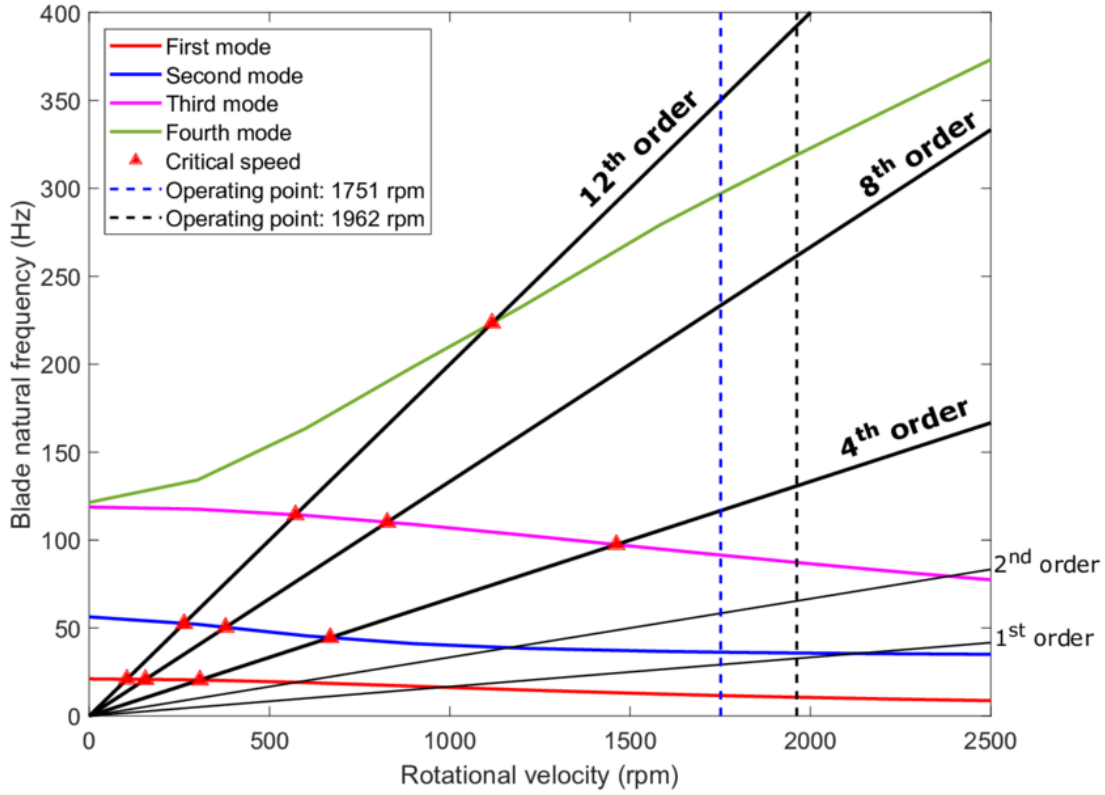

Figure 2.4: Campbell diagram with different engine orders responses [12]

an appropriate level of non rotating damping, and it is crucial to have the best possible balanced rotor.

Chapter 3

Rotordynamics modeling and analysis

Performing rotordynamics analysis can be quite useful during the design stage of a rotor system. While the study of an approximated model cannot totally replace the testing stage of the actual machine, it helps to find and fix possible design problems. The main objectives of this kind of analysis are:

- Predict critical speeds and define design modifications in order to change them in a way that they don't fall into the operational seed range.
- Predict natural frequencies of torsional vibrations.
- Predict threshold speeds and vibration frequencies for dynamic instability and determine design modifications to remove those instabilities.
- Predict amplitudes of synchronous vibrations generated by unbalance.
- Calculate balance correction masses and positions starting from measured vibration data.

3.1 Spring-mass model

3.1.1 Undamped system

The simplest model that can be used to perform vibration analysis is the single-degree-of-freedom spring-mass model, which is composed of a rigid mass mounted on a linear spring. The mass can only move in one direction, for example along the x-axis. In a freely vibrating system without external forces, being m the mass and k the stiffness of the spring, the equation that describes the motion of this system granting the dynamic balance of the mass is

$$m\ddot{X} + kX = 0 \tag{3.1}$$

This equation has two main possible solutions: the trivial solution $X(t) = 0$ describes the system at rest, while the solution of interest for the analysis is

$$X(t) = X_0 \cos(\omega t + \varphi) \tag{3.2}$$

This solution tells that the mass is subjected to an harmonic oscillatory motion, which is characterized by the three parameters:

- X_0 = amplitude,
- ω = pulse,
- φ = phase.

Pulse ω depends on the mass and stiffness of the system, while amplitude and phase depend on the initial conditions $X(0)$ and $\dot{X(0)}$.

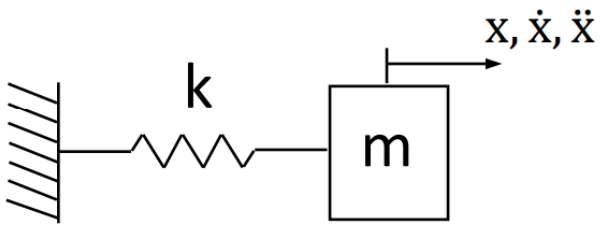

Figure 3.1: Single degree of freedom spring-mass model [13]

3.2 Jeffcott rotor

The spring-mass model can be used to approximate and understand the natural frequencies of the first mode of a rotor-bearing systems, but is very limited when it comes to more advanced analysis. First limitation is that, with one degree of freedom, this model can only execute a translational motion in a single direction, while the rotor-bearing system can perform whirl orbits with complex shapes. This limit can be partially solved by taking a system with two degrees of freedom, which is able to vibrate in two directions producing several different types of motion of the mass.
Another limit of the model, still present on the two degrees of freedom spring-mass model, is that it does not represent realistically the unbalance of the rotor. Since rotor unbalance is always present in real machines and since it is the cause of the most common type of vibration, it follows that unbalance is a necessary part of the basic model used for the analysis of rotating systems. This means that the center of mass of the disk does not coincide with its geometric center. The model obtained with these considerations is called *Jeffcott rotor model*, and consists of a rigid, unbalanced disk mounted on a uniform, massless, flexible shaft supported by rigid bearings.

Figure 3.3 shows a view of a whirling Jeffcott rotor, with the axis origin O at the shaft center, showing the shaft bending deflection given by the

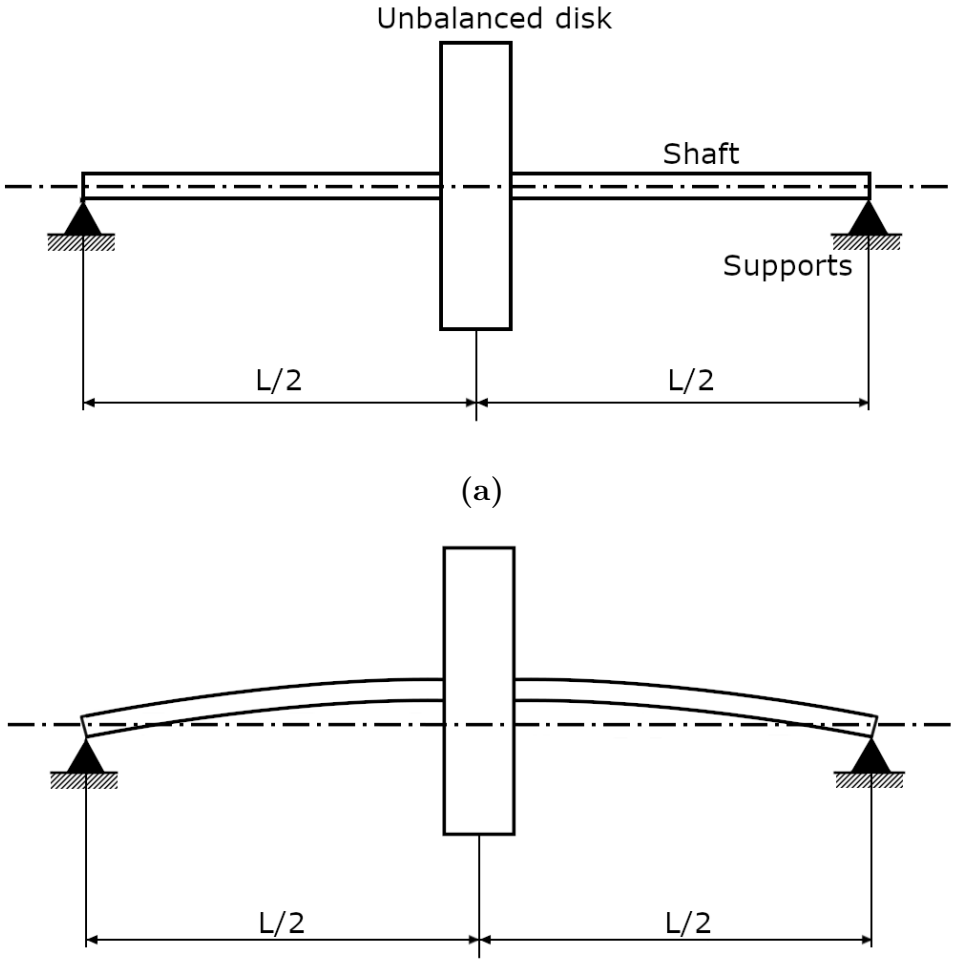

Figure 3.2: Jeffcott rotor at rest (a) and in displaced configuration (b)

dynamic loads ($\overline{OC}$). Being C the geometric center of the disk and G its center of mass, the static unbalance is $u = \overline{CM}$. θ is the angle between $\overline{OC}$ X axis, and its time rate is the whirl speed of the rotor ($\dot{\theta} = \omega$). φ is the phase angle, which is constant in case of synchronous whirl. The characteristics of the rotor are:

- k: bending stiffness of the shaft.

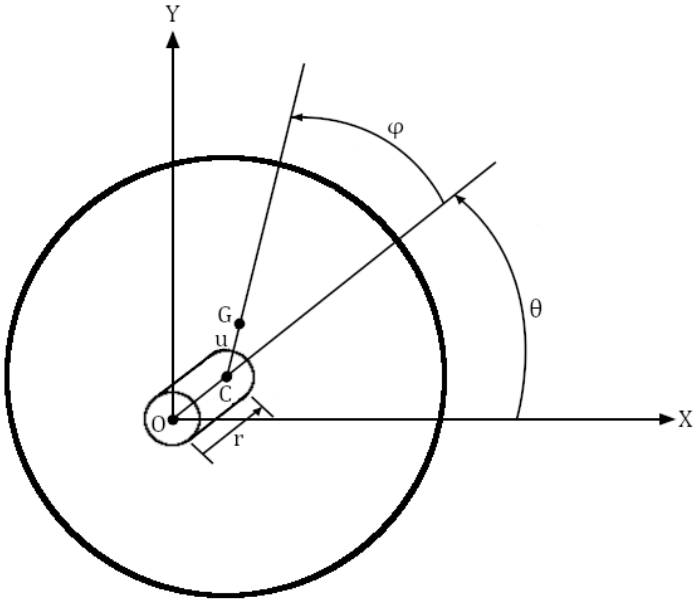

Figure 3.3: End view of a whirling rotor in displaced position

- m: mass of the disk.
- c: viscous damping given by the air drag on the disk and the shaft.

The system would have three degrees of freedom, but one is removed by assuming a constant speed. The solutions can be found in two different coordinates systems, polar or cartesian coordinates.

Polar coordinates

Polar coordinates (r, φ, θ) have the advantage of giving the solutions in term of amplitude and phase, which are of easier interpretation, but generate nonlinear equations of motion that are not well suited to study rotordynamics instability. These equations are:

$$\ddot{r} + \frac{c}{m}\dot{r} + \left(\frac{k}{m} - \dot{\theta}^2\right) r = \Omega^2 u \cos(\Omega t - \theta) \tag{3.3}$$

$$r\ddot{\theta} + \left(2\dot{r} + \frac{\dot{c}}{m} r\right) \dot{\theta} = \Omega^2 u \sin(\Omega t - \theta) \tag{3.4}$$

The solutions for synchronous whirling are:

$$r = \frac{\Omega^2 u}{\sqrt{(k/m - \Omega^2)^2 + (c\Omega/m)^2}} \tag{3.5}$$

$$\varphi = \arctan\left(\frac{c\Omega}{m(k/m - \Omega^2)}\right) \tag{3.6}$$

Cartesian coordinates

Cartesian coordinates X, Y and φ give way to linear equations and the displacements in term of X and Y are more similar to the way that those values are usually measured by the vibration probes. The differential equations of motion are:

$$m\ddot{X} + c\dot{X} + kX = m\Omega^2 u \cos(\Omega t) \tag{3.7}$$

$$m\ddot{Y} + c\dot{Y} + ky = m\Omega^2 u \sin(\Omega t) \tag{3.8}$$

Which gives as solution

$$X = \frac{\Omega^2 u}{\sqrt{(k/m - \Omega^2)^2 + (c\Omega/m)^2}} \cos(\Omega t - \varphi) \tag{3.9}$$

$$Y = \frac{\Omega^2 u}{\sqrt{(k/m - \Omega^2)^2 + (c\Omega/m)^2}} \sin(\Omega t - \varphi) \tag{3.10}$$

$$\varphi = \arctan\left(\frac{c\Omega}{m(k/m - \Omega^2)}\right) \tag{3.11}$$

It can be noted that it is possible to convert form cartesian to polar coordinates by observing that $r = \sqrt{X^2 + Y^2}$.

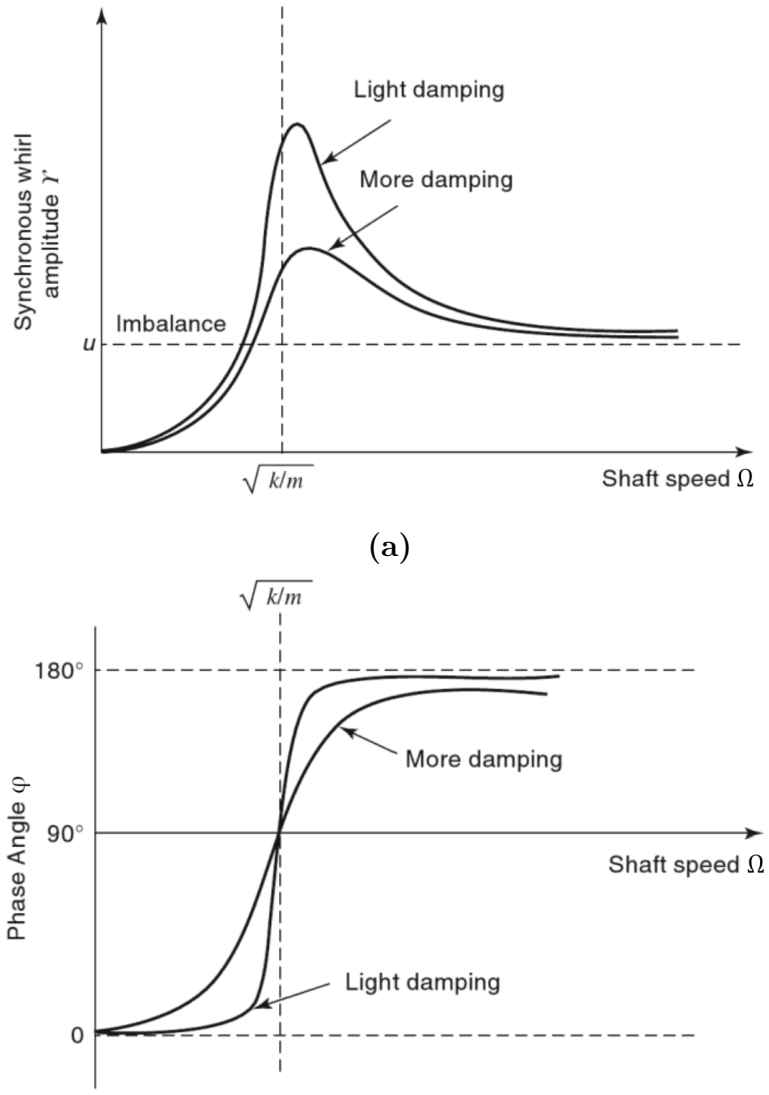

Figure 3.4: Imbalance response: amplitude (a) and phase (b) [5]

In figure 3.4 are shown the results of the Jeffcott rotor analysis. There can be seen an amplitude peak that correspond to the critical speed, as seen in chapter 2. Higher is the value of damping an lower will be the vibration peak. Also at the critical speed, phase angle passes through 90° and later reaches 180°. This indicates that the center of mass G, which was first rotating around the geometric center C, at higher speeds passes to the inside of the whirl orbit, thus having C whirling around G. This phenomenon is called *critical speed inversion* or *mass center inversion.* [5]

3.3 Beam model and 2D analysis

More complex models can be considered when dealing with rotordynamics analysis thanks to computer simulation. A common model, which is also the one used as an analytical aid during the work here presented, is the beam model. It can be seen as a 2D model, where the engine structure is represented by a network of beam type structural elements retaining the material and mechanical properties of the components they represent. This model has three main types of elements:

- Beam elements, these are the main elements of the model, each one of them representing a continuous structure with its stiffness, mass, inertia and also the eventual damping. The distribution of stiffness and mass can be defined in different locations, called stations, along a beam element.
- Springs, are used to represent short or geometrically complex structural components, such as bearings, engine mounts or damper elements. Springs depict the stiffness or the damping of these components, but, unlike beams, do not retain any information of mass or inertia.
- Joints, are elements used to link beams and springs together and to hold

the model in place. Usually every beam and spring must present a joint at each end.

Mass, stiffness and damping properties are given as matrices, in a similar way to what seen for the equation of motion in chapter 2. Such equation can be written in a simplified form (without the gyroscopic and circulatory matrices) as:

$$[M]\ddot{\mathbf{q}}(t) + [C]\dot{\mathbf{q}}(t) + [K]\mathbf{q}(t) = \mathbf{f}(t). \tag{3.12}$$

This is solved by the analytical program using different solving methods, depending on the kind of analysis requested. The mathematical details of the solution process will not be further elaborate, since they are complex and not relevant to the work at hand.

Different types of analysis can be performed using this 2D model. These can be dynamic analysis, such as critical speed, natural frequencies and forced response analysis, or static analysis like maneuver and static forces loads. The analysis are often linear, but nonlinear analysis can also be performed. The degrees of freedom considered are the translational and rotational ones. The axial and torsional degrees of freedom can be neglected for the purposes of unbalance response analysis.
This is true when working with simple rotors. It becomes less accurate when dealing with more complex systems characterized by three dimensional couplings between different rotors. Figure 3.5 shows a model of a simple rotor, with the spring elements that represent the supports onto which the rotor is mounted.

For the purposes of this particular study, the most used one has been of course the synchronous forced response analysis. This analysis allows to predict the behavior of the rotor at different rotational speeds, estimating,

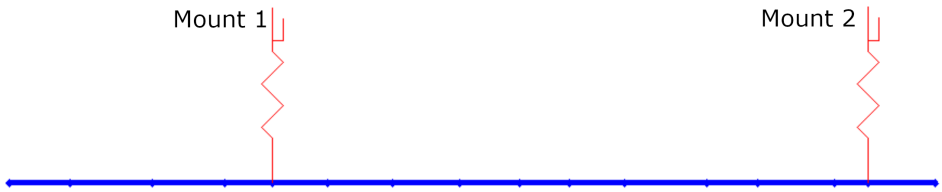

Figure 3.5: Example of a simple rotor seen as a beam model

for example, the resulting vibrations or the load on the mounting supports of the rotor. It is also possible to simulate a change in the unbalance of the rotor in order to study the effects.
Not having access to a enough actual test data during the development of the code, these kind of analysis have been particularly useful in the tool validation stage of the present work, allowing to simulate the balancing process on a rotor model to study the effectiveness of the solution obtained through the procedure.

Chapter 4

Test data analysis

4.1 Signal analysis

In this chapter are described the initial steps performed by the tool, starting from reading the raw test data given in input to obtain the unbalance response vectors. The tool has been developed using the Matlab environment and the graphic interface was generated through its built-in App Designer feature. It is able to read test data files with various extensions, like *.mat* and *.datx* files and Dewesoft's *.dxd* and *.d7d* files.

The first step of the balancing process performed by the tool consists in reading and analyzing raw data obtained through measurements taken on the running engine during field tests. These data are signals detected from sensors mounted in specific positions on the engine. There are different kinds of transducers that can be used to measure vibrations. In the specific cases studied during the development of the tool only two kinds of sensors were considered: accelerometers and the keyphasor transducer.

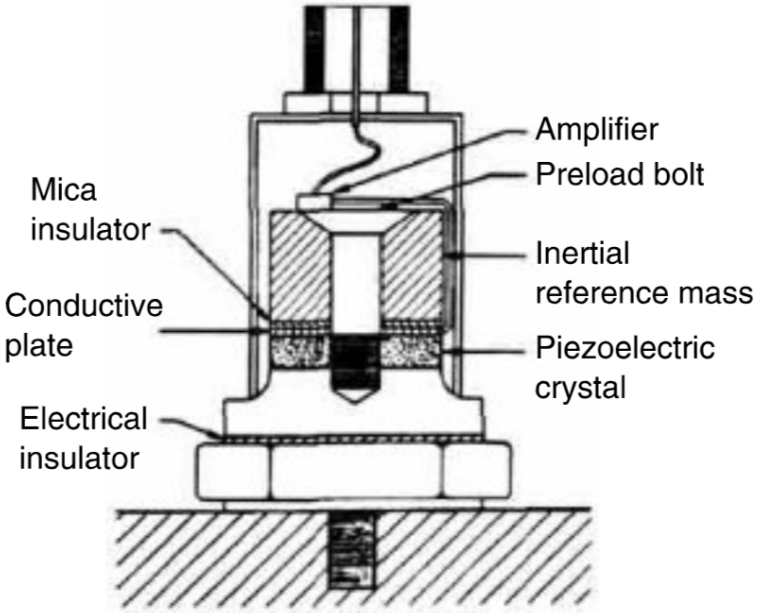

Figure 4.1: Piezoelectric accelerometer [8]

4.1.1 Accelerometers

Accelerometers are transducers that measure mechanical vibrations in terms of acceleration. They are the most common type of transducer used for mechanical vibrations measurements. [8]
Accelerometers can usually measure vibrations on a single axis. Depending on their orientation they can be used to detect radial or axial movements. Since rotor unbalance has mainly influence on the lateral mode, this paper will consider radial accelerometers, but the analysis and the considerations made should be the same for any other kind of vibration measured.

The accelerometers utilized in the tests analyzed are the ENDEVCO 2221F piezoelectric accelerometers. This kind of accelerometer is composed of inertial mass that exerts a force on the piezoelectric crystal proportional to the acceleration of the component on which it is mounted. The piezoelectric

Figure 4.2: ENDEVCO 2221F piezoelectric accelerometer [11]

crystal translates the applied force into an electric output analyzable by the acquisition system.
To get a better vibration measurement from the accelerometers they are usually used together with high impedance cables, which are coaxial low noise cables that grant better signal acquisition. Charge amplifiers are also typically needed, to amplify the accelerometer's response making it more easily readable.

Figure 4.3 shows the circumferential position, on the engine frame, of the three sensors utilized in the analysis of the test data available during the writing and testing of the balancing tool.

Raw data from the accelerometers contains all the measurable vibrations along the sensor's axis. They need to be processed in order to isolate the synchronous component which is the one given by rotor unbalance.

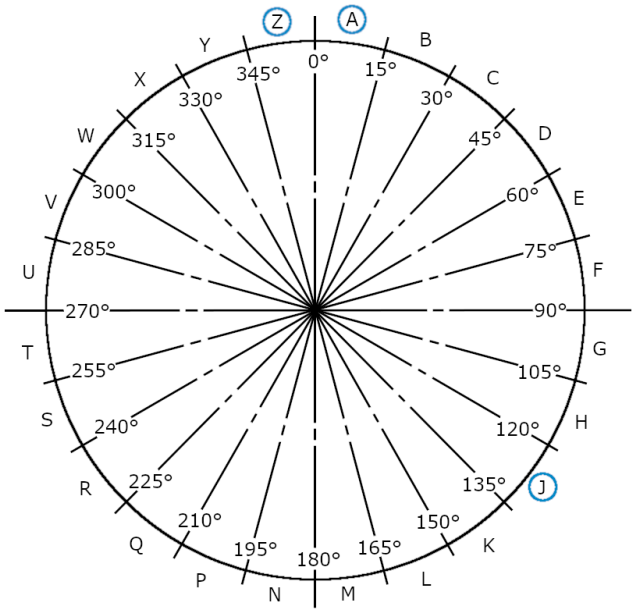

Figure 4.3: Circumferential position of the accelerometers with reference AFT Looking Forward

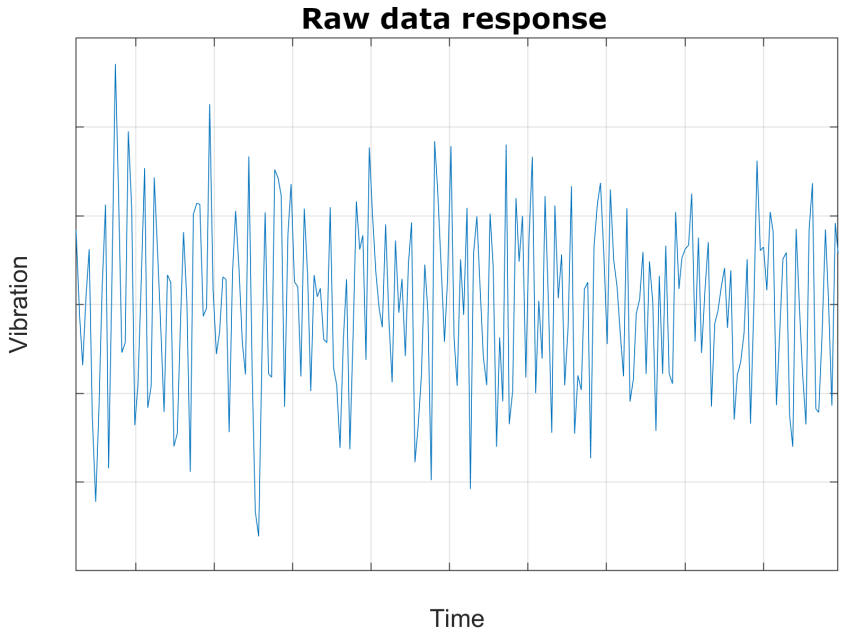

Figure 4.4: Example of vibrations measured by the accelerometers

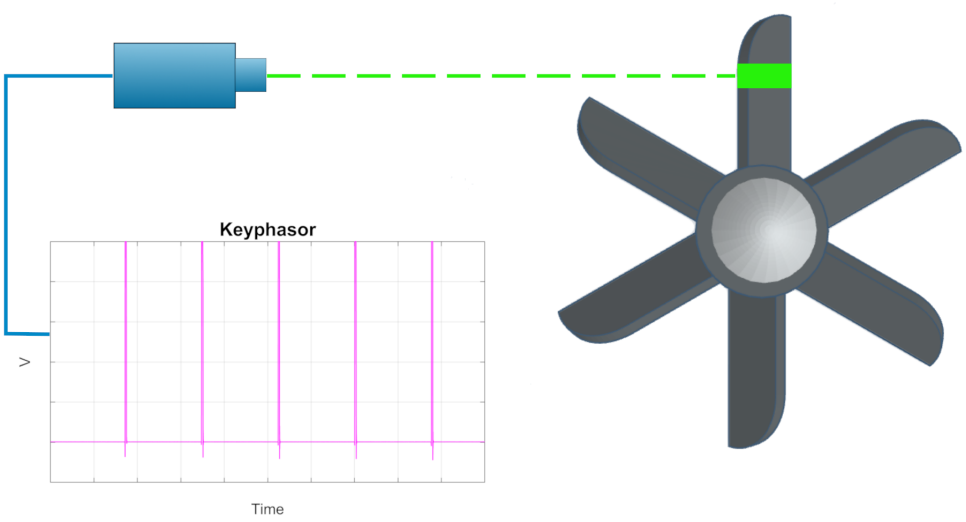

Figure 4.5: Keyphasor giving a once per turn signal to measure the blade speed and position

4.1.2 Keyphasor

The keyphasor transducer is a sensor that provides a once-per-turn signal by detecting a particular mark placed on the rotor. A common type of keyphasor consists in a proximity transducer that senses a discontinuity on the rotor, like a notch on the surface. In the presented case, were the rotor studied is the propeller, the keyphasor is a light sensor that detects a segment of reflective tape placed on the reference blade.
The signal generated is an on/off type of wave, with a positive impulse corresponding to every passage of the marked blade. This transducer plays two significant roles. It allows to measure the rotor's spin speed and to know the vibration signal phase, which is the relative position of the reference blade with respect to the vibration peaks.

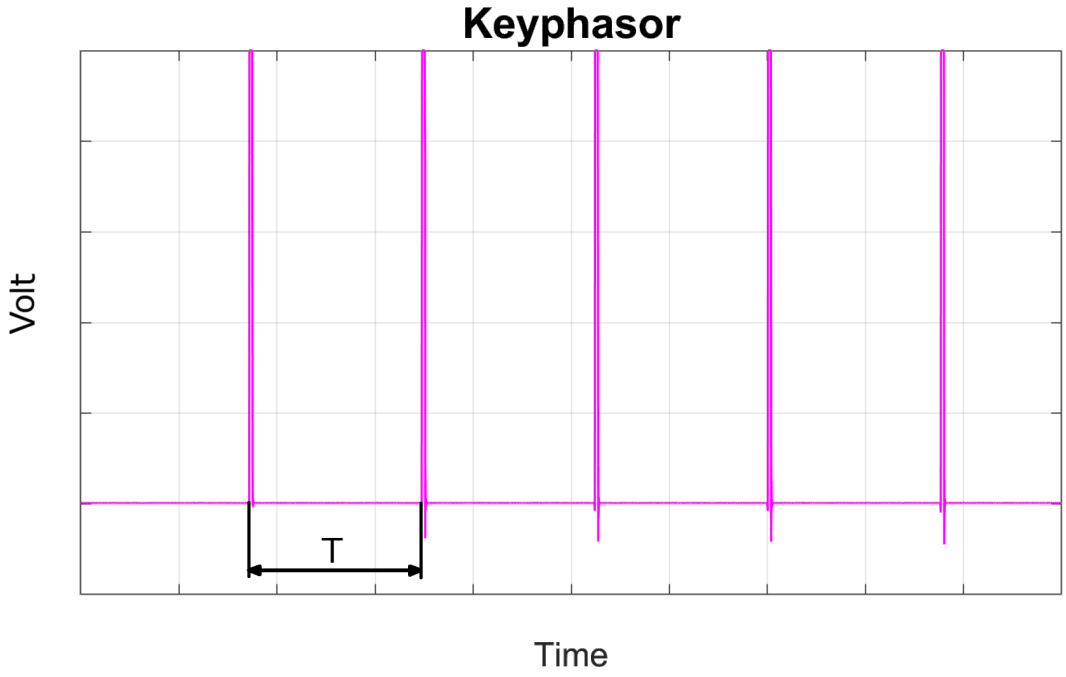

Figure 4.6: Keyphasor signal

4.2 Response vector calculation

The first step in the processing of the test data is measuring the rotor speed from the keyphasor, which is given as the frequency of the signal. To measure this frequency, the tool scans the signal in search of each impulse, storing the corresponding time values. The difference between each impulse time and the previous one is the duration T of that period. The frequency will then be equal to $f = \frac{1}{T_m}$, where T_m is the average of all the periods of the signal. The speed in RPM can also be found by multiplying f by 60.

Signal impulses are identified as the moment at which the keyphasor value passes over a certain threshold, defined by the user. A preview of the signal is available to evaluate the appropriate threshold to select. The tool analyzes the signal and proposes a threshold equal to the 75% of the maximum signal

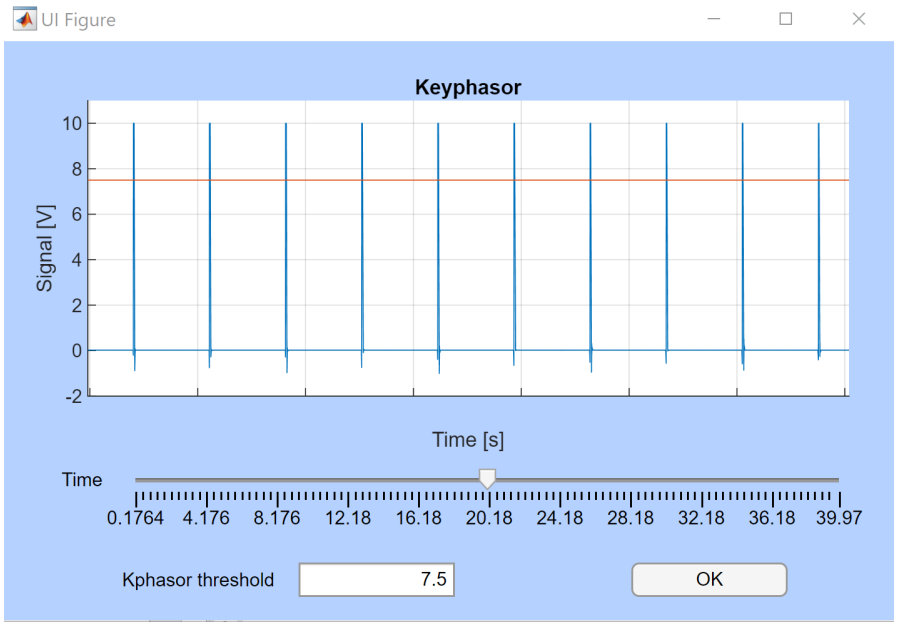

Figure 4.7: Keyphasor signal preview box

value. The user can then keep that suggested value or chose a more suitable one.

4.2.1 Filtered signal

Raw response data from the accelerators, as seen in figure 4.4, represent the actual vibrations of the system. It is a poly-harmonic signal composed by contributes given by the different forcing functions. In order to study the effects of unbalance it is necessary to isolate the synchronous component, which will be also called 1/rev, from the other components. This operation is done through a band pass filter with the passing band centered on the rotor spin frequency previously measured. The band pass is a filter that cuts out all the harmonic components of a signal which frequencies are outside of a defined range, leaving only the components with the desired frequency.

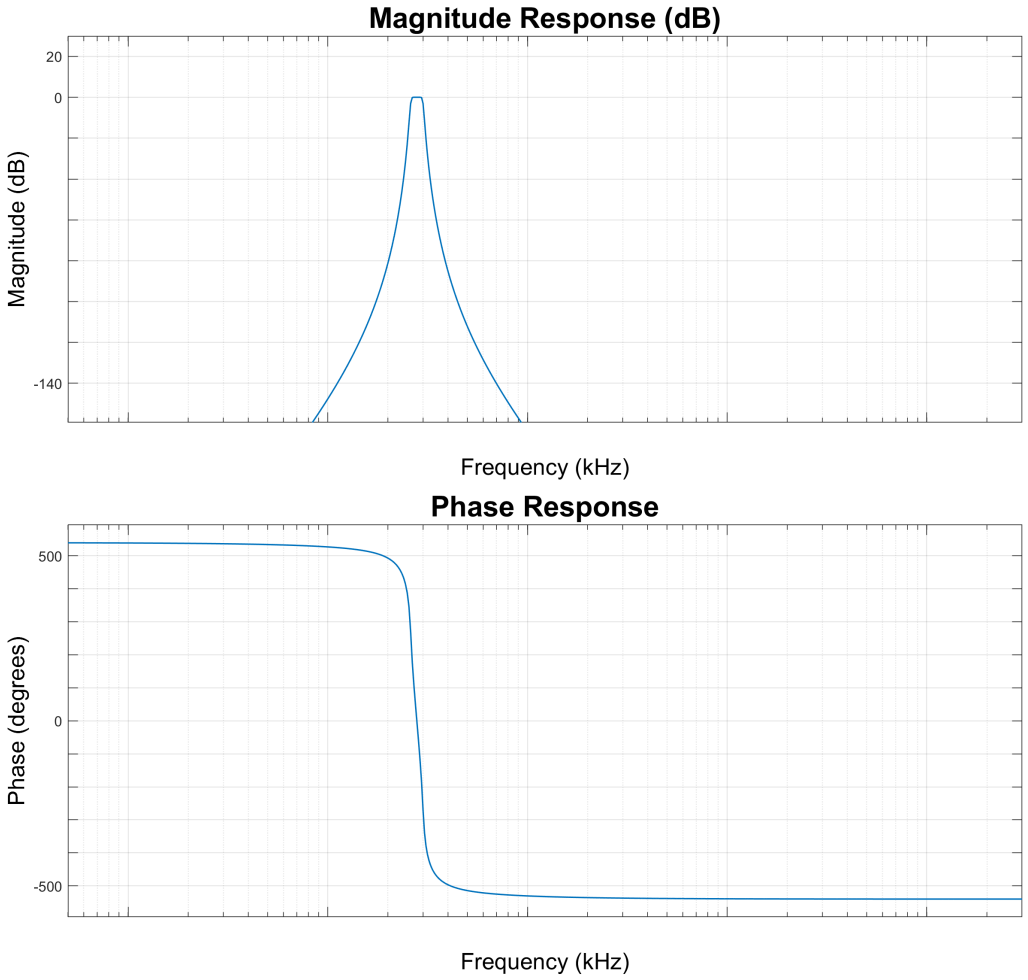

Figure 4.8: Band pass filter Bode plot

The bandwidth of the filter is given as an input by the user, as well as the filter order.

The filter order is the polynomial degree of the filter's transfer function. This parameter defines the steepness of the transition between the passband and the stopbands, thus effecting the attenuation of the frequency ranges adjacent to the passband. An higher-order filter results in a sharper and more effective filter. The downside, however, is that an high filter order can cause an high phase distortion, which is negative for the fidelity of the

resulting filtered signal. [9] A compromise between clean filtering and low phase distortion is needed, avoiding filter orders that are unnecessarily high.

The filter bandwidth defines the frequency range of the desired signal components. Everything outside that range has to be cut out by the filter. Since rotor's speed is never perfectly constant, choosing a bandwidth that is too narrow may results in missing parts of the 1/rev signal. On the other hand, a too large bandwidth would cause an undesired noise in the filtered signal.
The optimal bandwidth varies from one case to another, but the tests performed during the development of the tool suggest that it is usually quite narrow. In the examined cases a bandwidth in the order of less than 10 Hz was needed to obtain a good enough result without noticeable noise, and even 1 Hz could make the difference between an acceptable filtered signal and an unacceptable one.

The filter used by the tool is a Butterworth infinite impulse response (IIR) bandpass filter created with the command `designfilt`, which creates a digital filter using the given parameters such as the filter order, initial and ending frequency of the pass band (defined by the tool given the bandwidth and the rotational frequency) and the sample rate, which is usually read from the test data file.
The Butterworth filter is one of the simplest filter, which can maintain the same response inside the pass band at the growth of the filter order. Figure 4.8 shows an example of a bode plot of the filter utilized.

4.2.2 Phase calculation

With the 1/rev available, the next step is to measure its phase. This information tells the angular position of the vibration peak on the rotor,

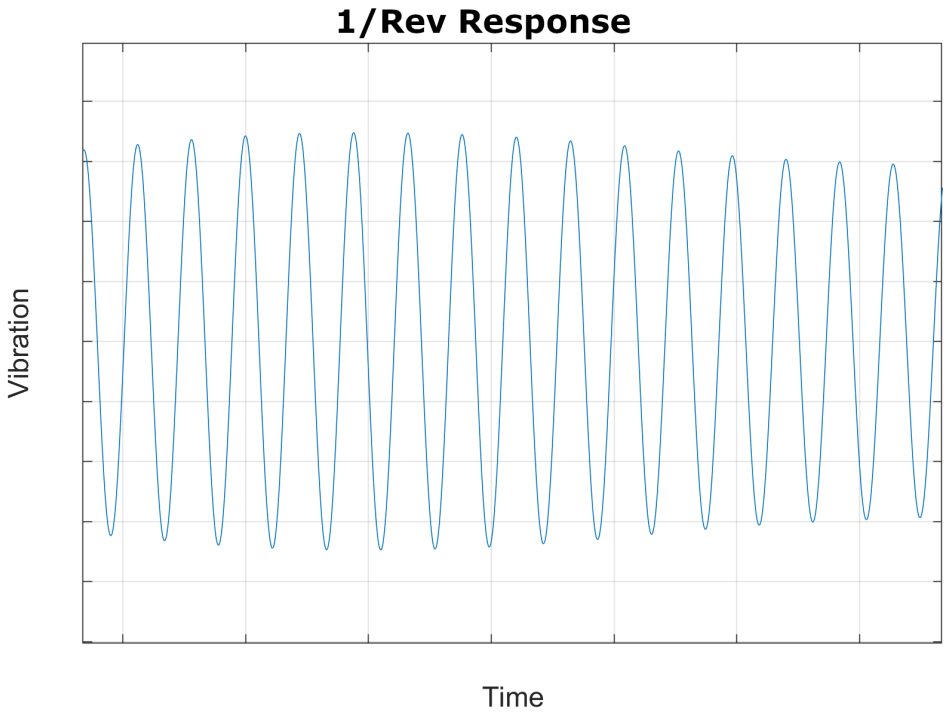

Figure 4.9: 1/rev filtered response signal

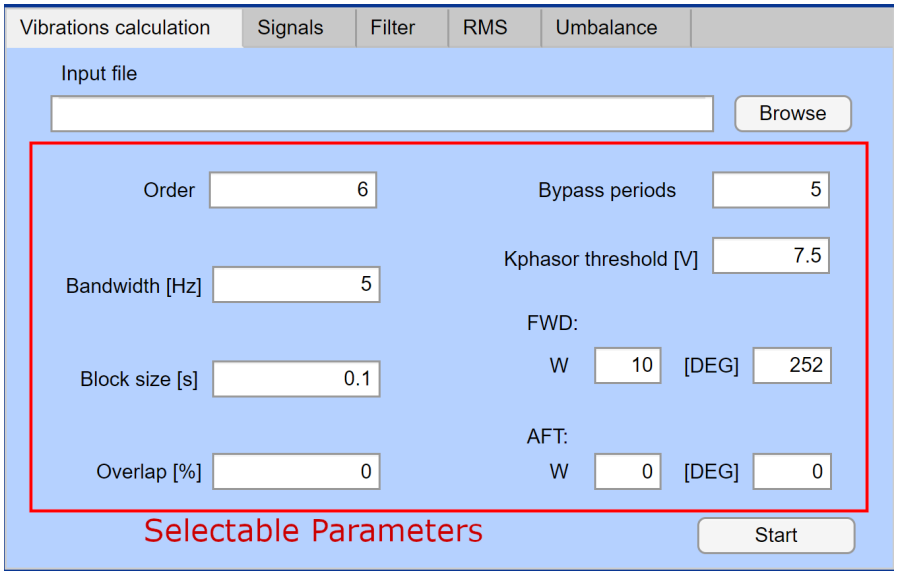

Figure 4.10: Analysis parameters selection window

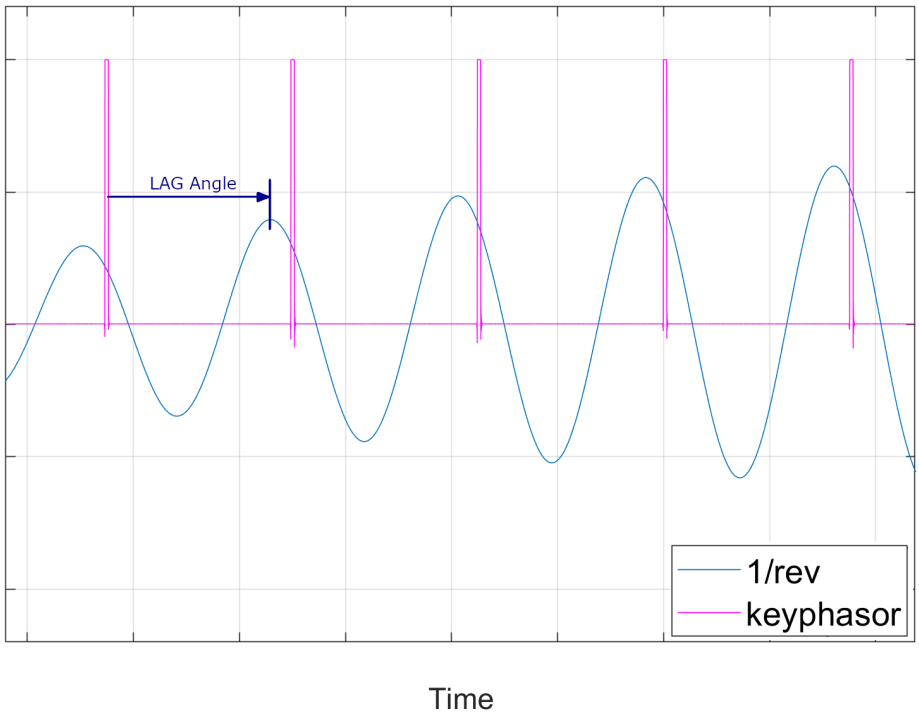

Figure 4.11: Visualization of phase lag convention

with respect to the reference blade. In this tool the phase is measured using the convention called *phase lag*, which means that it is given as the angle between the keyphasor impulse and the first occurring positive vibration peak, as visible in figure 4.11.

Using more analytical terms, the 1/rev phase for each period of the signal can be written in equation form as

$$\varphi = \frac{t_{1/rev} - t_{key}}{T} \cdot 360 \tag{4.1}$$

Where:

- $t_{1/rev}$ = time at which 1/rev peak occurs,

- t_{key} = time at which keyphasor impulse occurs,
- T = period duration.

The tool scans both the keyphasor and 1/rev signal, searching the respective peaks and storing the corresponding time into two vectors. The storing of these times begins after a number of initial periods has passed, since usually the starting transitory can introduce some errors. The number of periods to ignore is given by the user under the voice *bypass periods*, in the input parameters.
Since the phase lag convention starts from the keyphasor impulse, all the eventual 1/rev positive peaks found before that are ignored. Once all the peak times are stored, equation 4.1 is applied to find the phase value for each period.

It should be noted that, like rotor speed, the frequency of the 1/rev is not perfectly constant, which means that also the phase may slightly vary from one period to another. When the 1/rev phase is close to either 0° or 360°, the phase variation can result in the presence of two response peaks in the same keyphasor period, or the absence of a peak inside of a period. This condition can be approached in two different ways. The first solution consists in ignoring the irregular period, limiting the phase to the 0-360 degrees range and resulting in a phase jump from one endpoint to the other, as seen in figure 4.12a.

The second solution is to store every peak time for both signals, starting from the first keyphasor one, and compare each 1/rev peak with the corresponding keyphasor impulse. This way the resulting phase has a continuous evolution and it can assume values outside the range defined previously. The result is shown in figure 4.13. This solution allows an easier visualization and measurement of the average phase, which is the reason why it is the

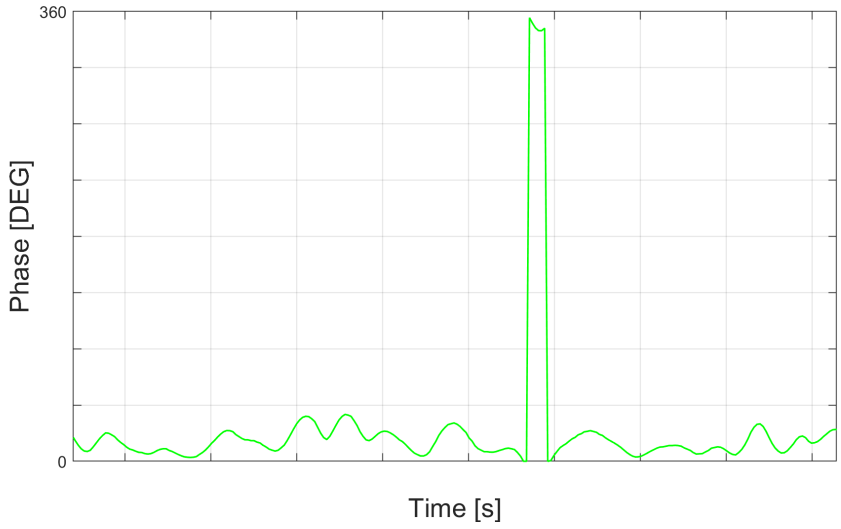

(a)

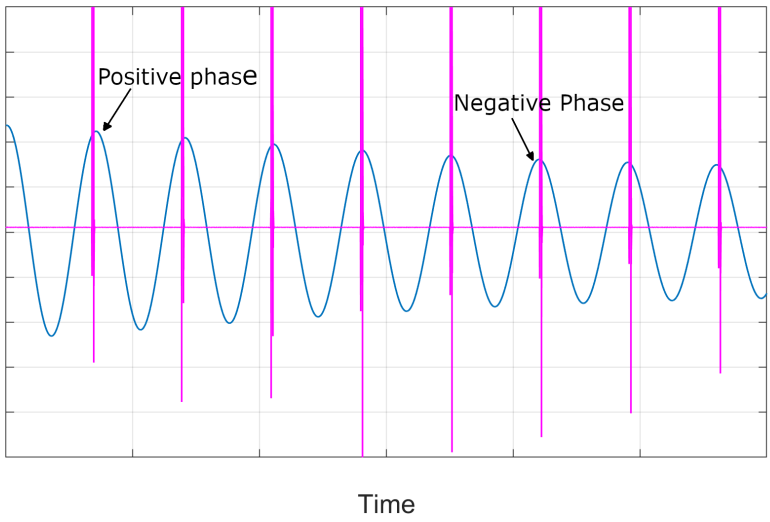

(b)

Figure 4.12: Phase discontinuity (a) and corresponding signal (b)

method applied for the purpose of this tool.

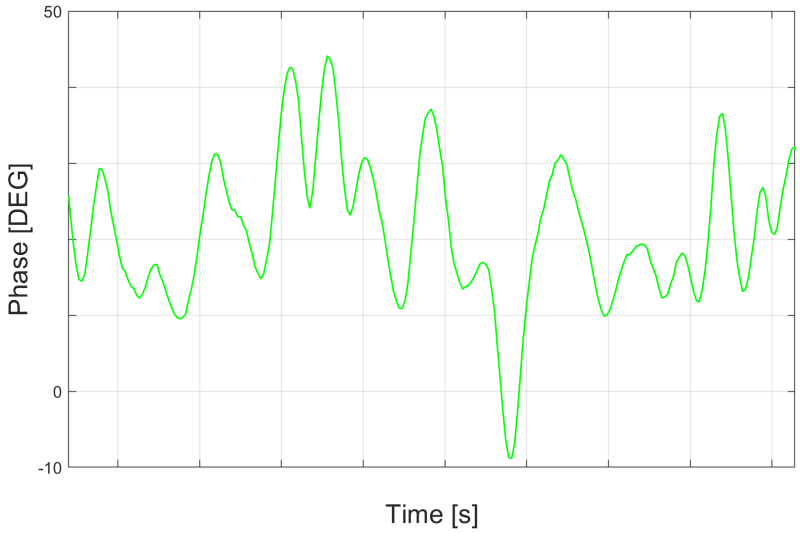

Figure 4.13: Same phase from figure 4.12a shown in continuous form

4.2.3 Amplitude calculation

The last step of signal analysis is to calculate the amplitude of the 1/rev response. It is computed by the tool as the root mean square of the signal (usually noted as RMS), which is defined as the square root of the mean square:

$$RMS = \sqrt{\frac{1}{N}\sum_{n=1}^{N}|x_n|^2} \tag{4.2}$$

were x is the considered signal vector.

The output needed from the analysis for the following steps of the balancing process is a single value of amplitude and phase of the response for each selected sensor, so the most immediate way to compute the amplitude would be to find the RMS of the entire signal. The tool, however, performs a block-based RMS calculation. It means that, instead of measuring the RMS of the entire 1/rev, it divides the signal in blocks of defined constant duration and finds the amplitude for each block. Using this more articulated

method allows to better study the evolution of response amplitude through time.

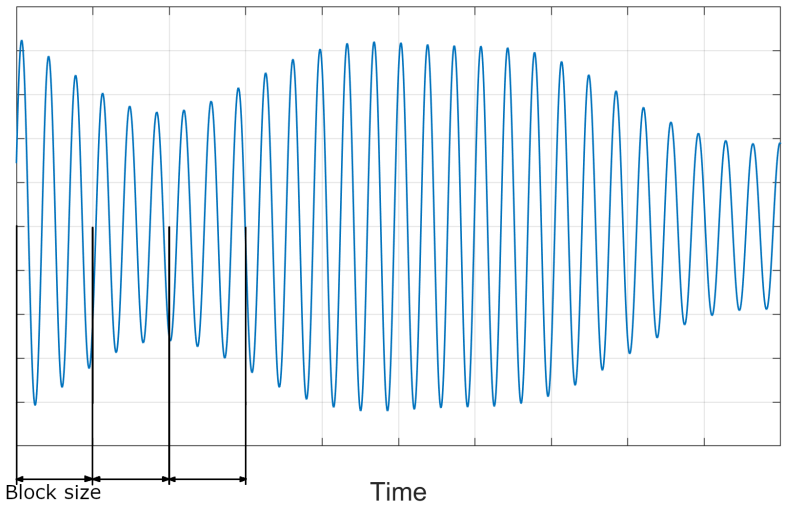

(a)

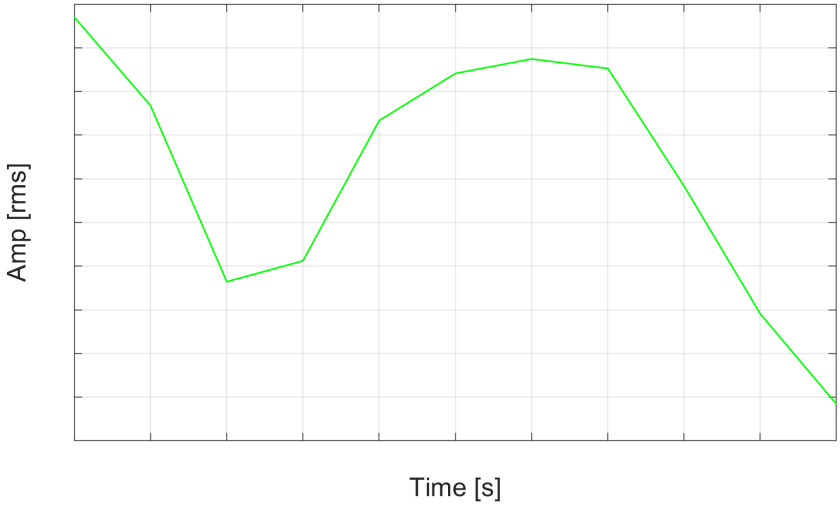

(b)

Figure 4.14: Block division (a) with corresponding RMS (b)

4.2.4 Output of the analysis

At the end of the signal analysis, the tool prints a plot that shows the evolution of amplitude and phase of the response, for each sensor, through time. An example of these plots is shown in figure 4.15. By looking at this output, the user is able to qualitatively evaluate the results in order to decide if the chosen input parameters are acceptable and if the selected sensors give a reliable and useful reading of the response.

Finally, a single value of amplitude and phase for each sensor, computed as the average value of the plotted results, is stored to be used in the following steps of the balancing process.

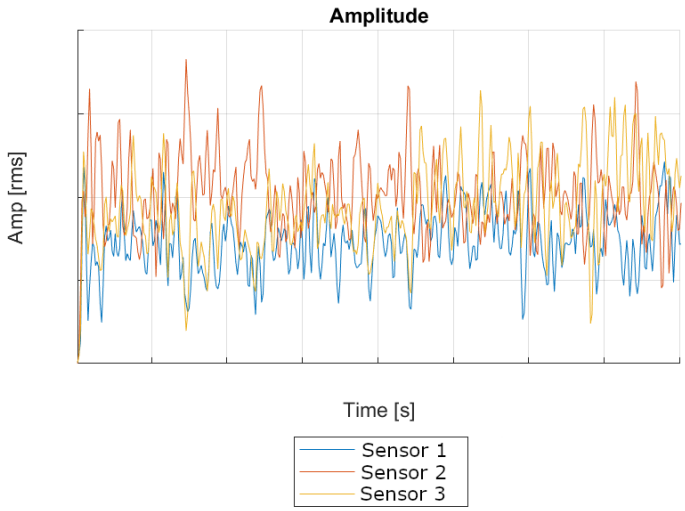

(a)

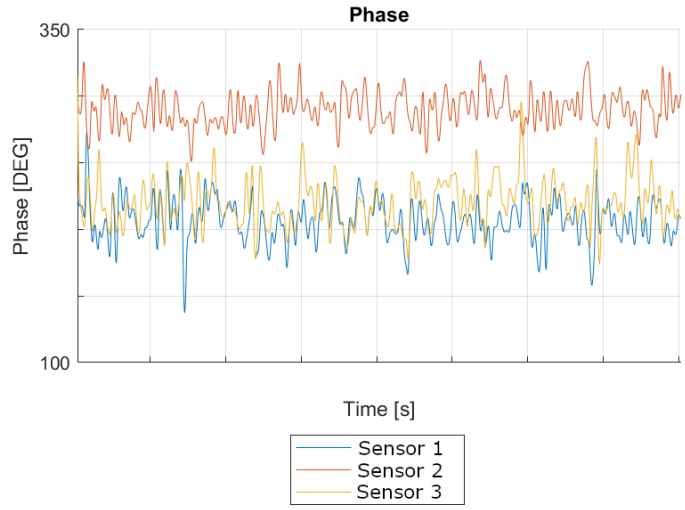

(b)

Figure 4.15: Response amplitude (a) and phase (b) plotted as output

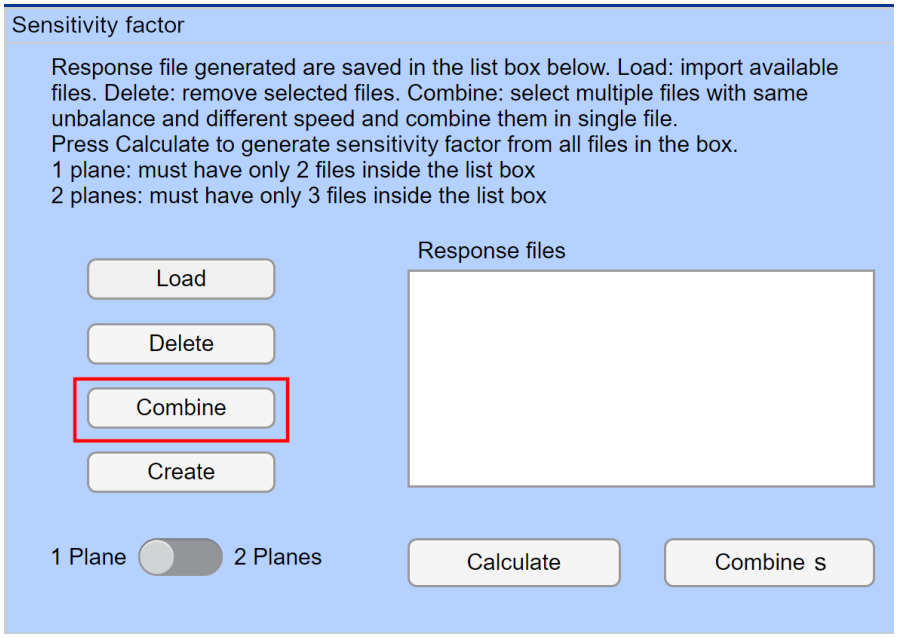

Figure 4.16: Sensitivity factor calculation window with buttons to interact with response files

4.2.5 Other response analysis features

At its current state, the tool has been mainly tested with test data with response signals measured at a constant rotor speed. Since the balancing process can be performed using measurements taken at different speeds for a better solution, a feature as been included that allows to combine different vibration response files. The code takes the selected available response files, scans them to find the sensors that are present in all of them and create a single file with only the response of said accelerometers at different speeds.

The tool was designed to operate not only with raw test data but also with already available response values given in polar coordinates as amplitude and phase. These data can be obtained by test data already processed using other tools or can be the result of an analysis performed on a model like the 2D analysis seen in chapter 3.

Figure 4.17: Response file creation panel

To easily input these data in a format that the tool can read and process a *create file* feature is available, which guides the user through the input process and gives a response file as an ouput.

Chapter 5

Balancing through sensitivity coefficient

Having measured the amplitude and phase of the 1/rev response is possible to further proceed with the balancing process. This tool uses the influence coefficient method. It is a balancing procedure that starts from considering the measured vibrations as a direct effect of concentrated unbalances placed on arbitrarily defined planes along the rotor's axis. This method comes from the assumption that the rotor's response to unbalance has a linear behavior. The unbalance vector was defined in chapter 3 as the vector u that connects the geometrical center of the rotor to its center of mass. The vector defined this way will now be referred as the *unknown* unbalance vector. A new vector W can be defined as the applied balancing weight, with its mass as vector magnitude and its circumferential position as phase. This vector W will be referred to as *known unbalance vector* or just unbalance vector when considered as an input data, while it will be called balancing weight when given as solution of the process.

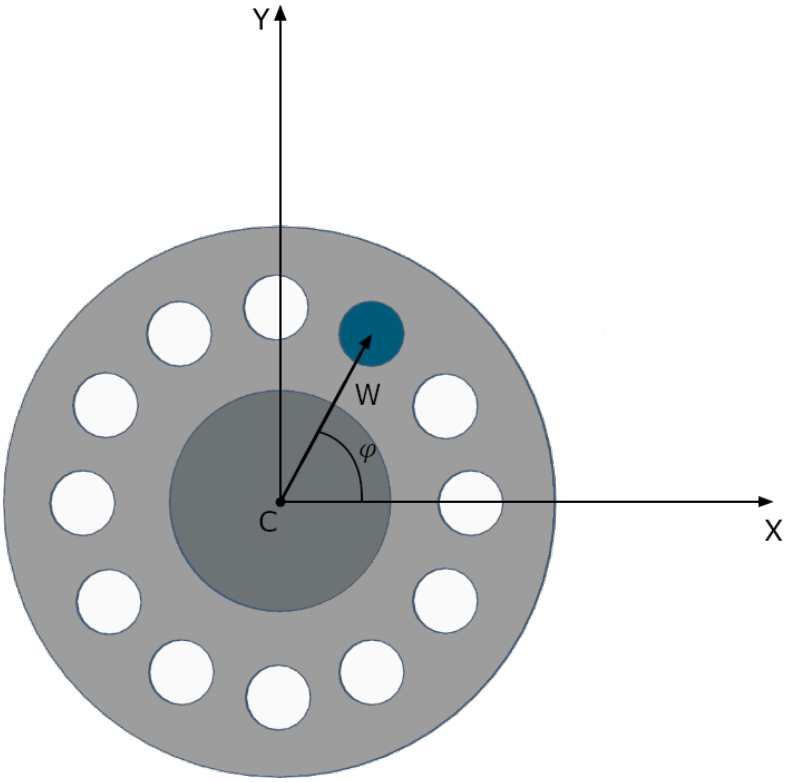

Figure 5.1: Unbalance vector Wt

To prevent confusion during mathematical passages, a further distinction can be made, by indicating with Wt the known unbalance vector applied and with W the balancing weight solution.

5.1 Sensitivity factor

The next step is to find the influence coefficient, also called *sensitivity factor*. It is the coefficient that allows to know the linear correlation between a certain unbalance vector and the 1/rev response.
In order to find the sensitivity factor for a determined rotor, performing a single test run is not enough. Having to define how the unbalance vector

affects the vibrational response, at least two runs are needed. The first run is usually called *baseline* and a simple test run of the rotor or engine that needs to be balanced.
The second run needed is called a *trial run* and consists on operating the same rotor of the first run under the same conditions, but with a trial balancing weight applied at a determined angle φ that represents the known unbalance vector. The trial run is the reason why the known unbalance vector as been previously defined as different from the balance weight solution.

In figure 5.2, vector V_0 is the initial vibration vector given by the baseline run and V_1 the response vector of the trial run, both represented as phasors in polar coordinates as seen in chapter 2.
The initial vibration V_0 represents the effect of the intrinsic unknown unbalance present on the rotor, while vector A represents the effect of the unbalance weight installed in the trial run.
The sum of these effects gives the response of the trial run V_1. Ideally, if A is equal to -V_0, the resulting response would be zero. With this method, balancing means finding the mass to add to the rotor in order to have $A = -V_0$. [6]

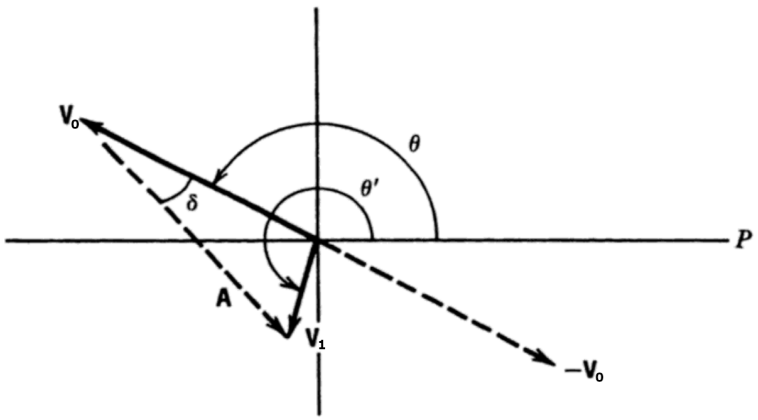

Figure 5.2: Graphical representation of a balancing vector solution [6]

5.1.1 Single plane

Single plane balancing is the simplest application of the influence coefficient method. It requires two test runs: the baseline and one trial run.

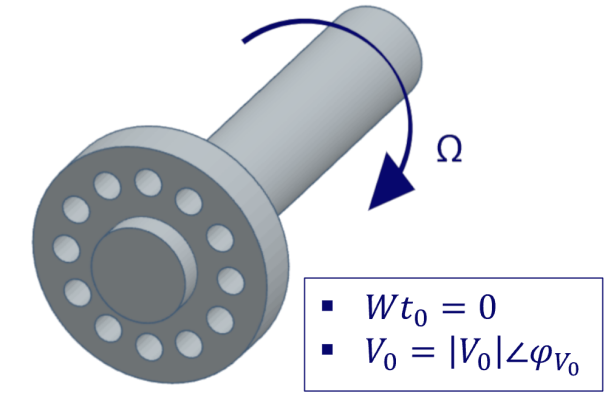

(a)

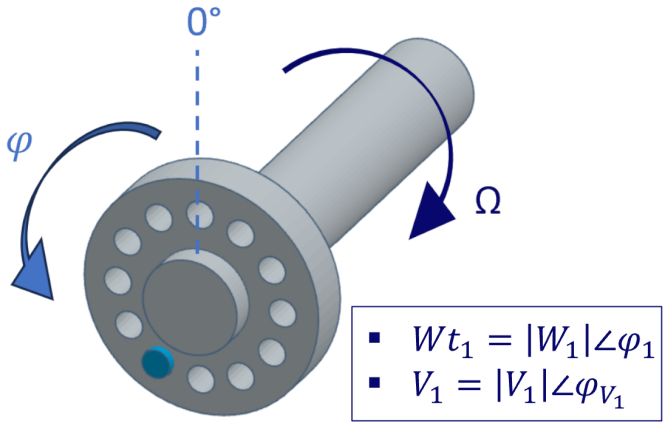

(b)

Figure 5.3: Baseline (a) and trial (b) rotor configurations

Note that, as shown in figure 5.3b, using the phase lag convention to measure the 1/rev response vector means that the phase angle φ is defined

as positive in the opposite direction of the rotor spin speed Ω.

The sensitivity factor for the single plane balancing is defined as

$$s = \frac{\Delta Wt}{\Delta V} = \frac{Wt_1 - Wt_0}{V_1 - V_0} \tag{5.1}$$

where:

- Wt_1 = known unbalance vector applied to trial run,
- Wt_0 = known unbalance vector applied to baseline rotor,
- V_1 = measured response of trial run,
- V_0 = measured response of baseline run.

The baseline run usually has an unbalance vector Wt_0 equal to zero, but by considering the vector difference ΔWt this is not strictly necessary. The sensitivity factor can also be measured between two runs both performed with weights applied, as long as the two unbalance vectors are different.
As seen in chapter 4, response analysis usually considers data from multiple sensors.
In addition, the same configuration can be run at different rotor speeds and the response vector from the same sensor has to be measured separately for each speed. Equation 5.1 gives the coefficient referring to a single speed-sensor combination. The balancing of the rotor can be made at the speeds for which there is a known sensitivity coefficient. A sensitivity vector defined at more rotational speeds allows an easier balancing at the varying of these speeds.

Until this point the vectors have all been considered in polar coordinates as amplitude and phase, but from equation 5.1 going forward they will be

converted in complex numbers for the purpose of performing calculations, since this allows an easier computing of the equations. The output values, however, will still be visualized in polar coordinates, which is far more intuitive for the end user to read.

The sensitivity factor is a coefficient that has to be applicable on every rotor that belongs to the same family. Which means that every rotor that is designed in the same way should ideally give the same sensitivity factor, no matter what kind of unbalance is applied.
This is the strength of the sensitivity coefficient method, because, once the sensitivity factor for a determined kind of rotor is available, all the following similar rotors can be balanced by using the same coefficient, without having to repeat the entire process. With a sensitivity factor already available, the only thing needed is a test run of the baseline rotor that needs to be balanced.

5.1.2 Two-planes balancing

The case previously considered refers to a single plane balance condition, which means that the balancing weight is placed only on one plane perpendicular to the rotor axis.
Generally, the balancing of a rotor can be made using multiple balancing planes, each one at a different axial position and each one with a different balancing mass applied. The tool developed has been limited to a maximum of two balancing planes, placed one at the front end, noted as FWD, and one at the rear end of the rotor, noted as AFT.

In order to generate the sensitivity factor for a two planes balancing, data from a second trial run are necessary, for a total of three test runs. Both planes must have a weight change with respect to the baseline in the two

trial runs, each trial introducing at least one weight change on a different plane that the other. This means that if the first trial run has a weight change on one plane, the second trial has to have a weight change on the other plane.
If one of the trials has weight changes on both planes the other trial must have at least one plane with an unbalance vector that is different from both the baseline and the first trial run.
With two balance planes and three weight configurations, there are a number of different possible combinations. These combinations can be divided into two main cases: an ideal case and a general case.

The sensitivity factor for a two-planes balancing consist of two coefficients for each speed-sensor combination: one that describes the effect of the FWD plane on the response and one for the AFT plane. The solutions for the two cases defined are described as follows.

Ideal case

The ideal case, represented in figure 5.4, is the one that presents the most immediate solution for the sensitivity factor. It includes a baseline run with no weights applied on any of the two planes, one trial run with weight applied on just the FWD plane and the other trial run with weight applied only on the AFT plane. This can be denoted as the ideal solution because it is the most intuitive way to perform the three test runs needed for the balancing process.

Under these conditions, the sensitivity factor for the FWD plane can be found using equation 5.1 with data from the baseline and the first trial, in the same way seen for the single plane solution. Similarly the sensitivity coefficient for the AFT plane is obtained using the data from baseline and

the second trial.

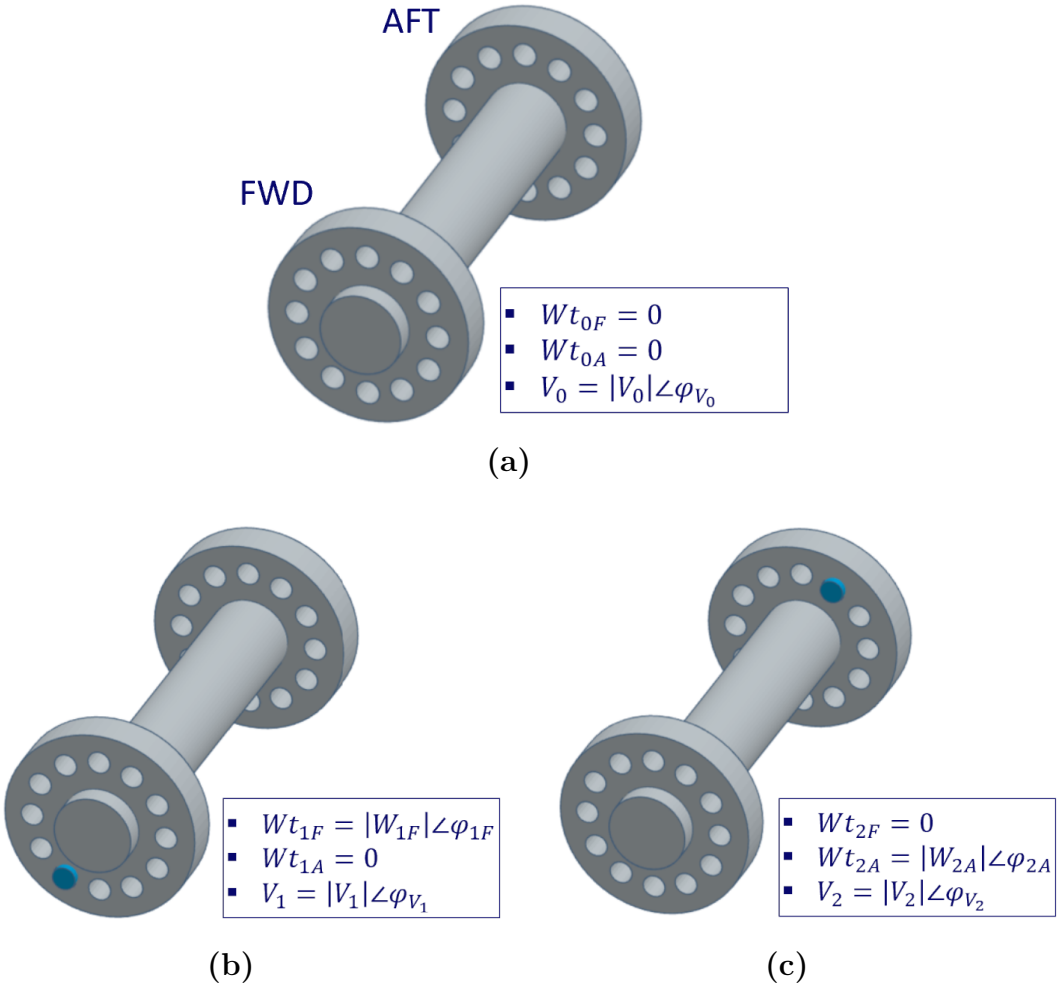

Figure 5.4: Baseline (a), trial 1 (b) and trial 2 (c) rotor configurations for the ideal case

General case

There could be situations, for example when dedicated engine test can not be made and the balancing has to be performed with available data, where the solution seen above is not valid. This happens when one or both the trial test runs have a weight change, with respect to the baseline, on both the balancing planes. When this happens, the rotor presents two unbalance

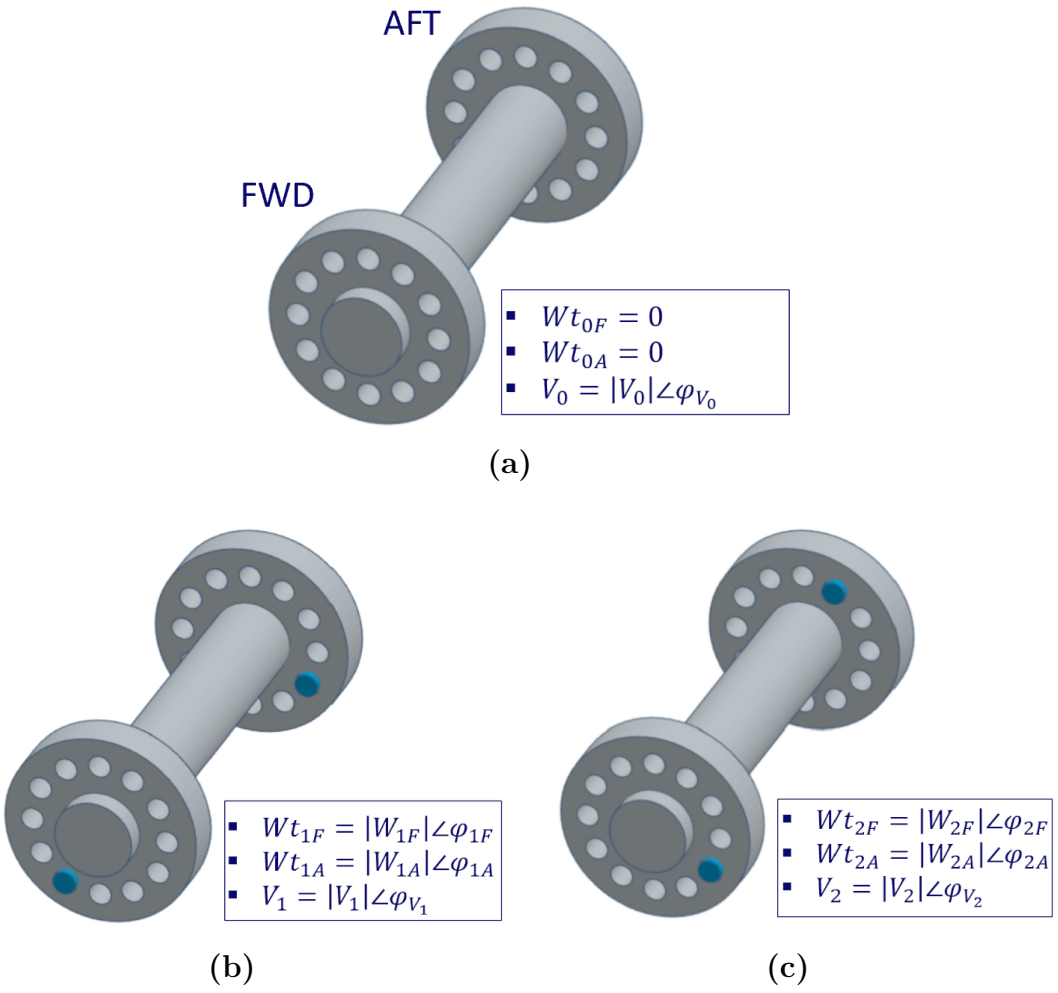

Figure 5.5: Baseline (a), trial 1 (b) and trial 2 (c) rotor configurations for the general case

vectors that produce a single response vector, which is a combination of the effects given by both planes. To find the sensitivity factor, however, it is necessary to know the component of vibration caused by each plane.

The following solution is denoted as a general solution, since it can be applied to any weight combination on the three configurations, with the only exception of the case in which two of the three test runs are performed under the exact same weight configuration. This solution applies also on the ideal case, which is the reason why it is the only method used in the tool for the two-planes case.

The sensitivity factor for a generic two-planes balancing case can be found by imposing the following system

$$\begin{cases} Vu_{1F} = \dfrac{Wt_{1A} - Wt_{0A}}{-s_{AFT}} + V_1 = (Wt_{1A} - Wt_{0A}) \left(-\dfrac{Vu_{2A} - V_0}{Wt_{2A} - Wt_{0A}} \right) \\ s_{AFT} = \dfrac{Wt_{1A} - Wt_{0A}}{Vu_{1A} - V_0} = \dfrac{Wt_{2A} - Wt_{0A}}{Vu_{2A} - V_0} \\ s_{FWD} = \dfrac{Wt_{1F} - Wt_{0F}}{Vu_{1F} - V_0} = \dfrac{Wt_{2F} - Wt_{0F}}{Vu_{2F} - V_0} \\ Vu_{2F} = \dfrac{Wt_{2A} - Wt_{0A}}{-s_{AFT}} + V_2 = (Wt_{2A} - Wt_{0A}) \left(-\dfrac{Vu_{1A} - V_0}{Wt_{1A} - Wt_{0A}} \right) \end{cases} \tag{5.2}$$

Where:

- A and AFT refer to the AFT plane,
- F and FWD refer to the FWD plane,
- Indices 0, 1 and 2 refer respectively to baseline, trial 1 and trial 2,

- Vu represents the part of the response given by the correspondent unbalance vector.

The first and last equations are used to find the portion of response caused by the unbalance on the front plane, respectively for trial 1 and trial 2. They are found by considering that, knowing the corresponding sensitivity factor, the response component generated by a given unbalance vector is

$$Vu = \frac{\Delta Wt}{s} \tag{5.3}$$

and being the total response V the sum effect of the two planes the vibrations caused by the front plane can be written as

$$Vu_F = V - Vu_A = V - \frac{\Delta Wt_A}{s_{AFT}} \tag{5.4}$$

As previously said, the sensitivity factor has to be valid for rotors with the same design, no matter what the unbalance is. This implies that, for each plane, both trials have to generate the same result. This equivalence of sensitivity factor between the two rotors is imposed by the central equations of the system.

By solving the system of equations the tool is able to find the sensitivity factor for a case with two balancing planes.

5.2 Best balance solution

The last step of the process at study is to find the weight solution that best balances the rotor. This solution is given as the weight W that results in

the lowest *residual vibrations*, which are the response to unbalance of the rotor after a certain weight is applied. These are given by the equation

$$V_r = \frac{1}{s}W + V_0 \tag{5.5}$$

Where V_r is the residual vibration and V_0 is the initial response vibration of the baseline, which is the rotor to balance. Having multiple response measurements from different sensors and at different speeds, possibly with influence from multiple planes, this equation is converted in matrix form

$$\{V_r\} = [S]\{W\} + \{V_0\} \tag{5.6}$$

Being m the number of sensors times the number of speeds and n equal to the number of planes:

- Vectors $\{V_r\}$ and $\{V_0\}$ have dimension m,
- Vectors $\{W\}$ has dimension n,
- Matrix $[S]$ has components equal to $\frac{1}{s}$, with s that has dimensions $m \times n$.

The solution W of equation 5.6 that minimizes V_r is found by the tool as the least square solution of the system obtained by imposing the residual vibration vector $\{V_r\} = 0$

$$[S]\{W\} + \{V_0\} = 0 \tag{5.7}$$

The least square solution of this linear system is

$$\{W\} = ([S^*]^T[S])^{-1}(-[S^*]^T)\{V_0\} \tag{5.8}$$

Where $[S^*]^T$ is the conjugate transpose matrix of $[S]$. This is a first weight solution that can be applied to balance the rotor. A prediction of the resulting residual vibration is made using equation 5.6.

A better balance solution can be obtained using an iterative process. The resulting solution obtained at the end of the iterations should be the optimized one that best reduces the residual vibrations on all the considered sensors. The ultimate solution is displayed by the tool with two values:

- the first solution is the weight to add to the rotor balanced in case the rotor has already a trial balancing weight,
- the second solution is the weight to apply if the weights previously present on the rotor are removed.

In case the balanced rotor did not have weights previously applied the two solution are intuitively equals. The tool also prints a report file containing information on the initial vibrations, the sensitivity factor used and the result of every iteration performed, included the residual vibrations predicted.

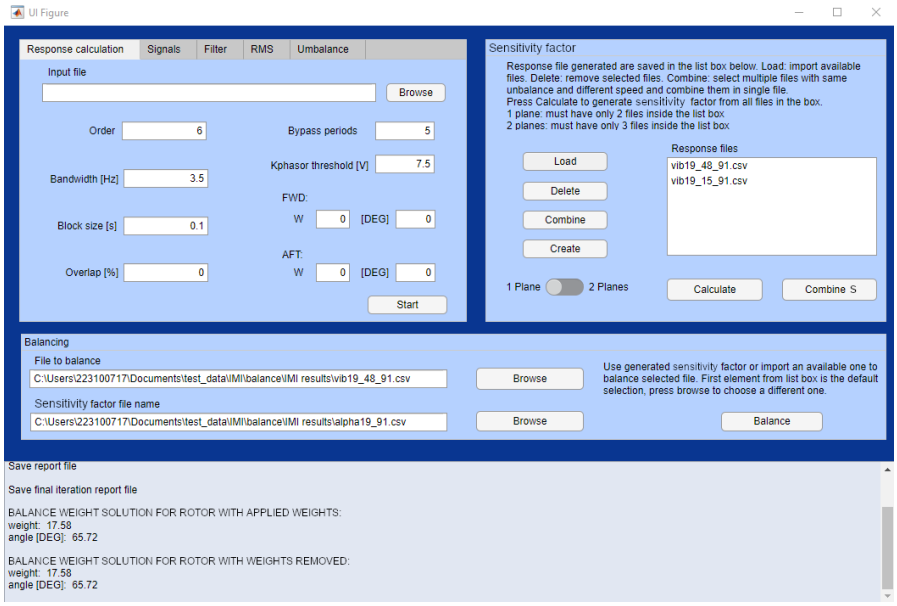

Figure 5.6: Tool interface with solution displayed

Chapter 6

Testing and validation of the tool

The tool was tested and validated by using it to perform three different types of balancing. The first two were balancing of 2D modeled rotors, while the last one was performed using available test data.

6.1 Two planes balancing

The analytical tests where made using the simple rotor model shown in figure 6.1. To this model are applied three different internal unbalances, each one

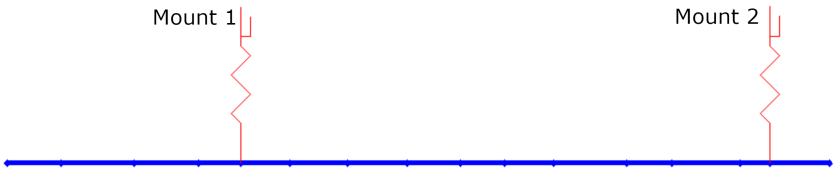

Figure 6.1: Rotor model used for 2D analysis

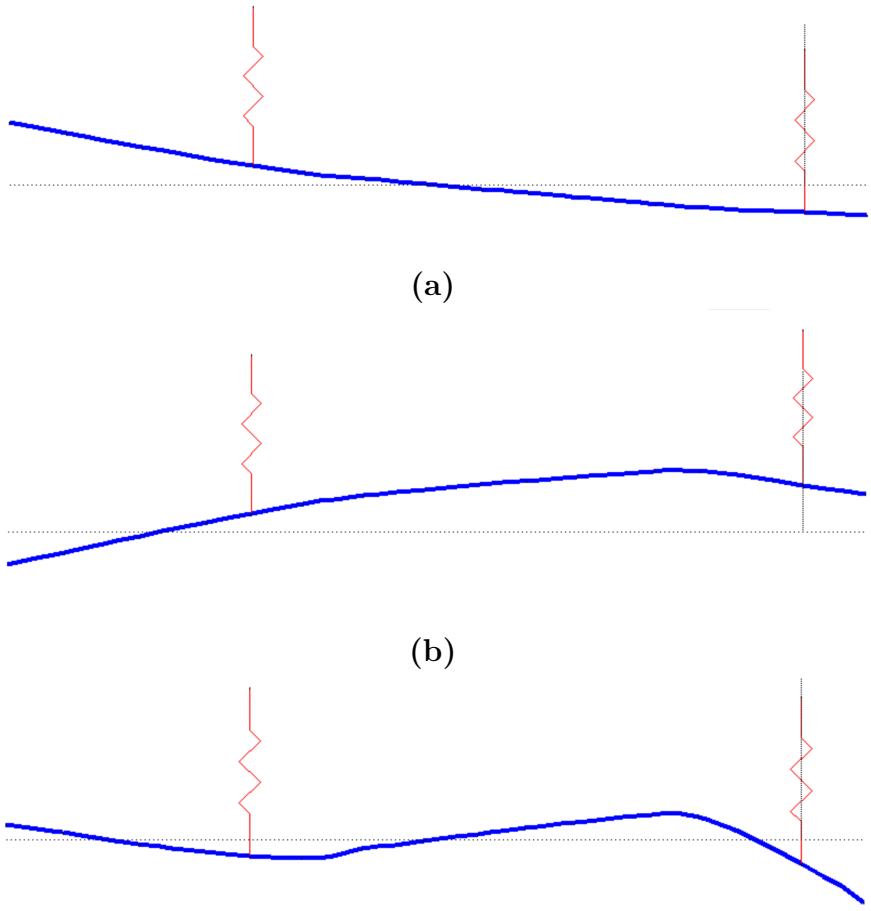

(a)

(b)

(c)

Figure 6.2: Displaced rotor corresponding to mode 1 (a) mode 2 (b) and mode 3 (c)

exciting a different mode at three different critical speeds: low frequency, middle frequency and high frequency.

The first test is a balancing made on two planes. Three different unbalances have been applied to the rotor, each one exciting one of the first three modes of the rotor. An attempt at balancing the three modes at a single operative speed (2000 RPM) has then been made. Each mode is balanced

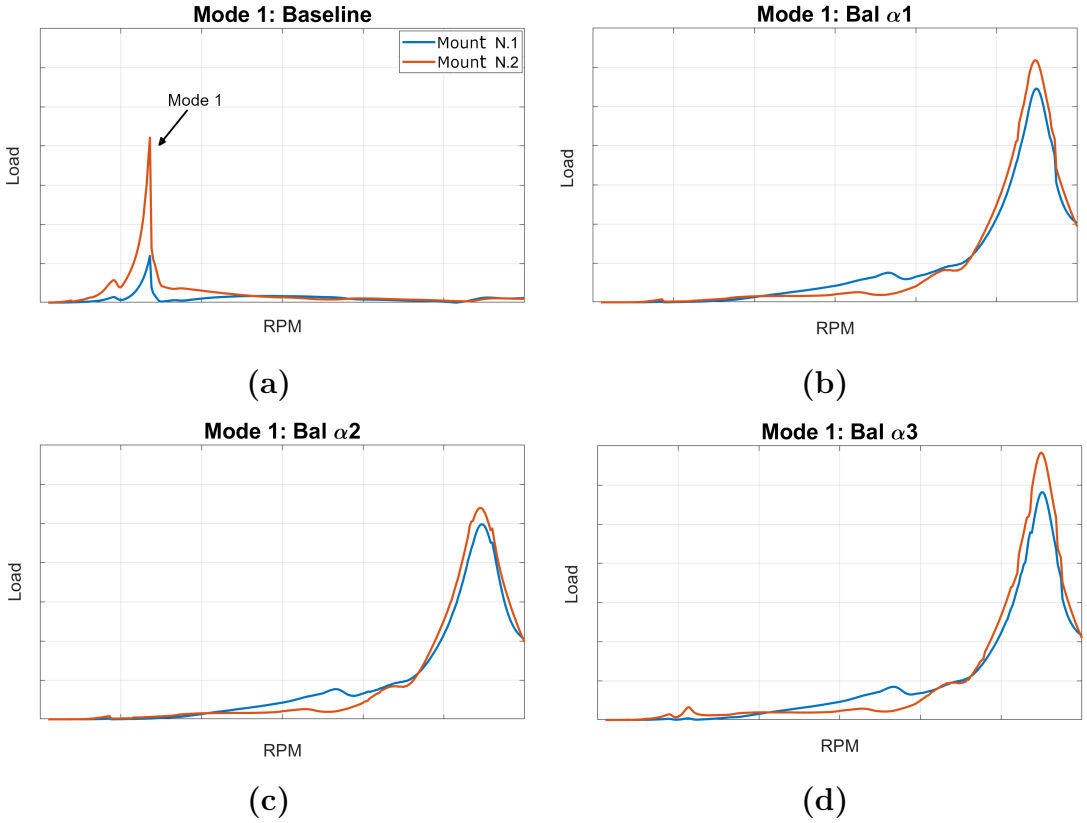

Figure 6.3: Baseline response of mode 1 rotor (a) with the responses resulting from balancing respectively with s_1 (b), s_2 (c) and s_3 (d)

three times, first using the correspondent sensitivity factor and then using the factors obtained for the other two modes, and the results are compared to define if a sensitivity coefficient calculated on a rotor can be effectively used to balance other similar machines.

The reason why the balancing is done at 2000 RPM and not at the critical speed is because it is a simulation of a test in which the rotor is tested isolated on a testing machine, which cannot reach the operational spinning speeds of the final engine. In this analysis, instead of the vibrations, the response measured is the load on the supports through which the rotor is mounted on the machine.

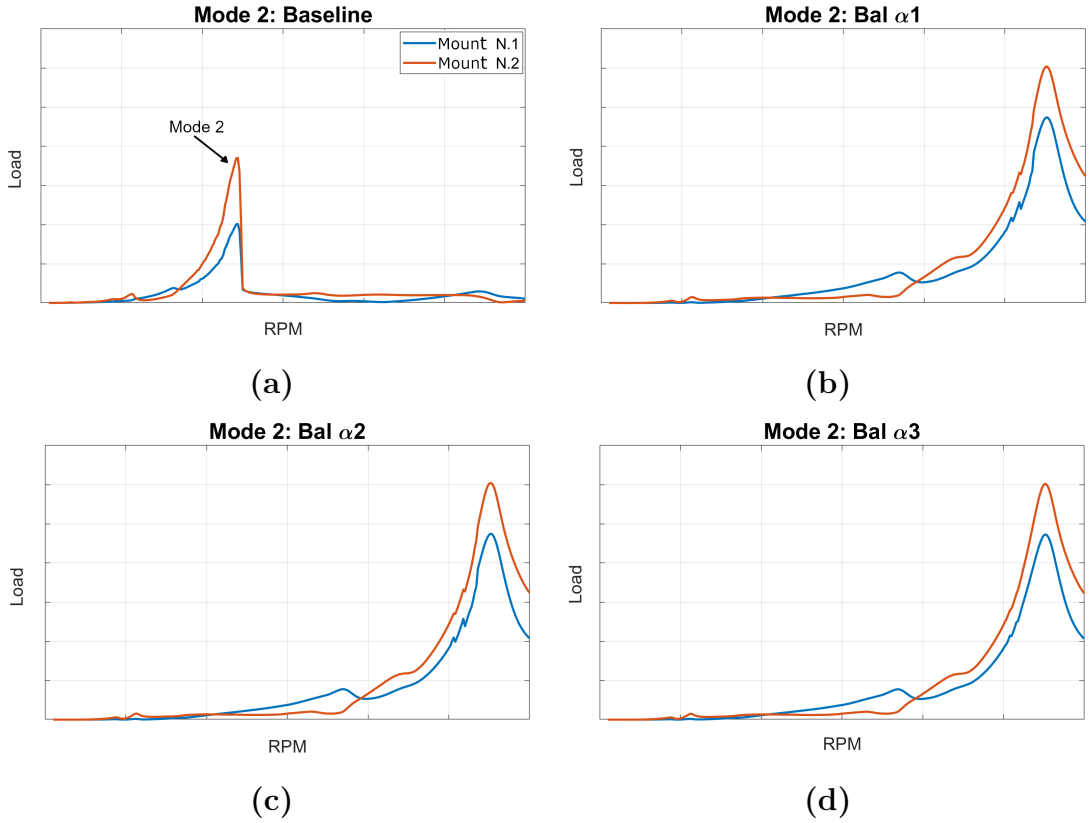

Figure 6.4: Baseline response of mode 2 rotor (a) with the responses resulting from balancing respectively with s_1 (b), s_2 (c) and s_3 (d)

Defining s_1 the sensitivity factor obtained using the rotor in which mode 1 (LF) is excited, s_2 the one for the rotor corresponding to mode 2 (MD) and s_3 the one corresponding to mode 3 (HF), the results of the analysis are shown in the following pages.
The results in figures 6.3, 6.4 and 6.5 show that, as predicted, the balanced responses are similar enough regardless of which sensitivity factor is used. Figures 6.3 and 6.4 also show that, for both the low frequency and the middle frequency modes, the balancing allows to highly reduce the response at the critical speed considered. The attenuation of the interested mode, however, causes an amplification of the high frequency mode on both cases.

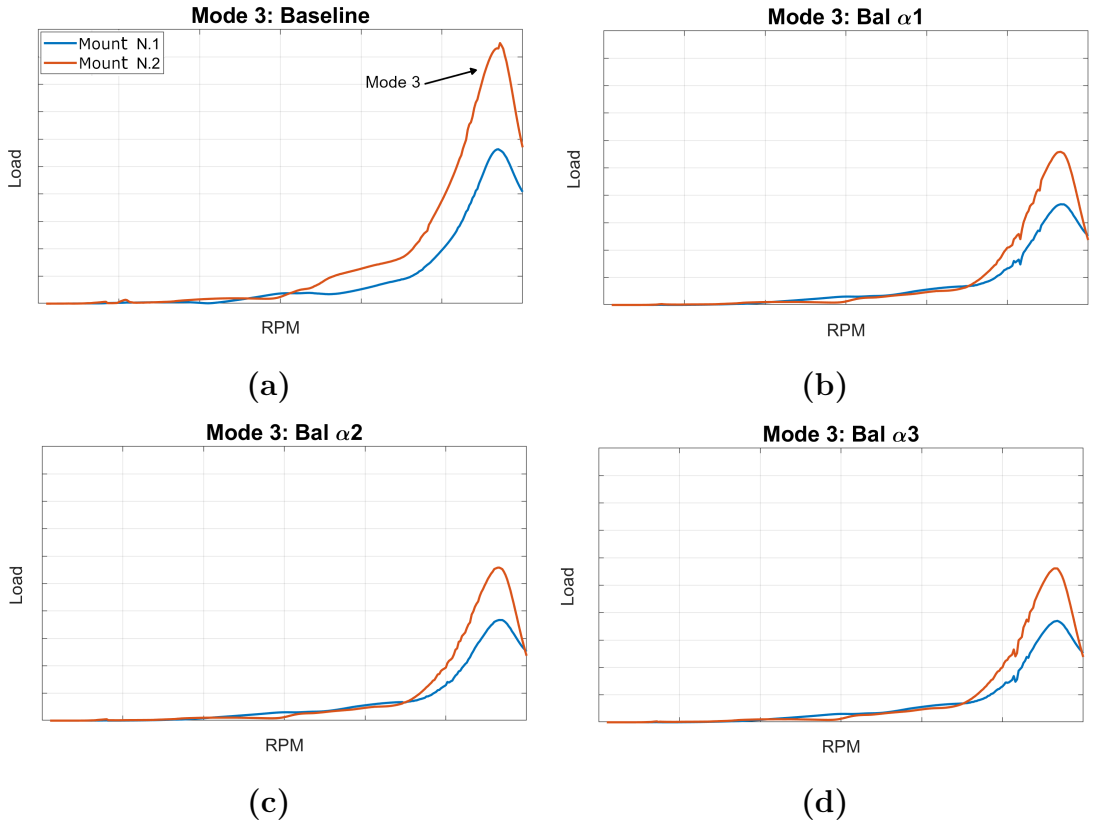

Figure 6.5: Baseline response of mode 3 rotor (a) with the responses resulting from balancing respectively with s_1 (b), s_2 (c) and s_3 (d)

By looking at figure 6.5, it can be noted that the balancing applied on mode 3 is not quite effective as it was on the two other cases, no matter what sensitivity factor is applied. The amplitude of the peak is reduced, but the mode is still significant. To analyze the reason of this issue, another test was made, by balancing the third mode using a sensitivity factor calculated using the response at its critical speed.

From the results obtained with this last analysis, shown in figure 6.6, it appears that balancing the high frequency mode at the critical speed has the desired effect, even though the response at lower frequencies is amplified,

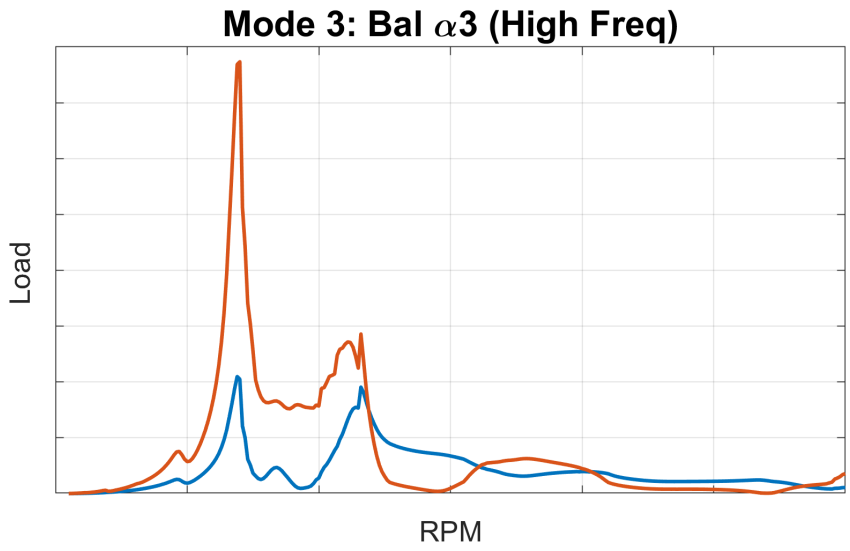

Figure 6.6: Response of mode 3 rotor after balancing at its critical speed

inversely to what happened with the other modes.
The conclusion that can be drawn from this result is that the failed balancing of figure 6.5 was not due to a failure of the tool, but more probably caused by the fact that the initial response at low speeds was too contained to allow an effective balancing of the high frequency mode using the sensitivity factor obtained at 2000 RPM.

6.2 Trim balancing

The second 2D analysis takes the same three initial rotors, with the three different modes excited. The objective, this time, is to balance each mode with the sensitivity factor obtained at its corresponding critical speed, considering the vibrations predicted by the model in three locations representing three different sensors mounted on the rotor. This is a simulation of a balancing performed using test data from the rotor mounted on the entire engine and

only one balancing plane is considered, since the second could be difficult to reach in this conditions.

The results of this second analysis, pictured in figures 6.7, 6.8 and 6.9, show that the single plane balancing at the critical speeds as a similar effect to the one seen in the previous case. Once again, figures 6.7 and 6.8 show a significant reduction of the interested modes, with the drawback of a strong amplification of the high frequency mode.
Figure 6.9 depicts the balancing of mode 3. Even though its curve is not flatten out at high frequencies, unlike what happened for the two planes balancing, the response presents a good reduction of the vibration.

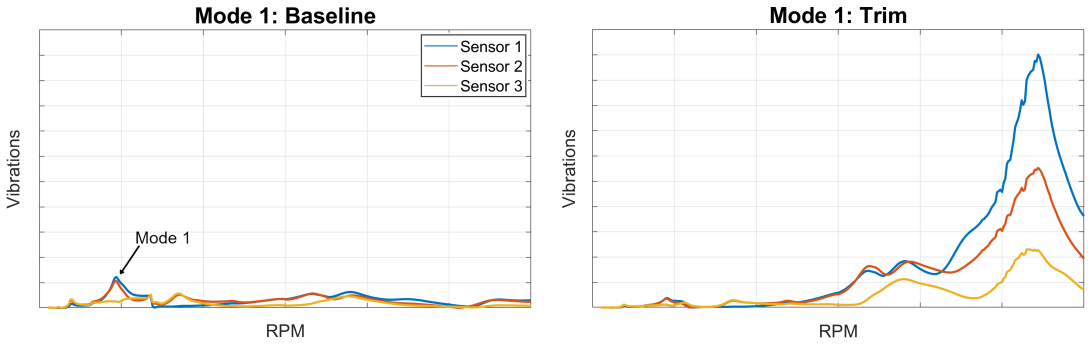

(a) **(b)**

Figure 6.7: Baseline response of mode 1 rotor (a) with the responses resulting from balancing (b)

Additionally, the amplification of the lower modes caused by the balancing is considerably more contained than the one obtained in the previous test.

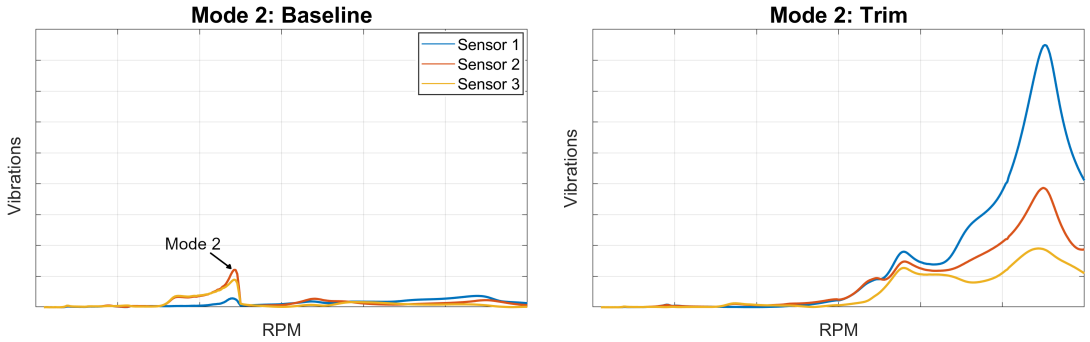

(a) (b)

Figure 6.8: Baseline response of mode 2 rotor (a) with the responses resulting from balancing (b)

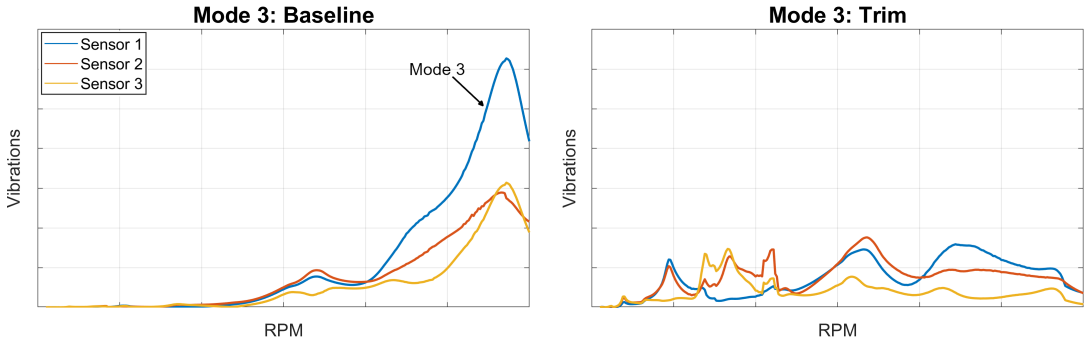

(a) (b)

Figure 6.9: Baseline response of mode 3 rotor (a) with the responses resulting from balancing (b)

6.3 Validation through test data

The third test performed to validate the tool is a balancing of the propeller of an existing turboprop engine of which there were test data available. The weights applied to each run are reported in table 6.1. There is only one weight applied for each run and they are all on the same plane, so the analysis is a single plane balancing. This mean that the three data file are not used together during the process but only two at a time.

Table 6.1: Weights applied on the different test runs

Test run	Mass	Angle
	gr	DEG
Baseline	0	0
Trial 1	10	252
Trial 2	8.6	162

Since there was not a test run of the balanced rotor available, it was not possible to compare the results from the tool with an already tested solution. The validation was then made by finding the balance solution of three possible combinations of these runs and comparing the results to see if they are at least similar to each other. The three combinations studied are:

1. sensitivity factor from baseline and trial 1 and balancing of baseline,
2. sensitivity factor from baseline and trial 2 and balancing of baseline,
3. sensitivity factor from trial 1 and trial 2 and balancing of trial 1.

The results from these tests are presented in figure 6.10. The solution of interest is the one highlighted, representing the weight to add when all other eventual weights are removed, since the last test was made by balancing a trial run with a weight installed. There can be seen that the solutions for the three data combinations are similar but not perfectly identical.
This is justified by the fact that in a actual test run there are some factors that cannot be controlled and that cause slight changes on the responses even in two runs performed with the same identical configuration. Considering this, the differences between a solution and the other ones is small enough to be acceptable. The tool can then be considered as correctly working.

```
Best rotor balance solution:
weight mass:  17.58
weight angle [DEG]:  65.72
```

(a)

```
Best rotor balance solution:
weight mass:  20.00
weight angle [DEG]:  64.95
```

(b)

```
Best rotor balance solution:
weight mass:  16.56
weight angle [DEG]:  66.90
```

(c)

Figure 6.10: Balance solutions from tool for combination 1 (a), 2 (b) and 3 (c)

6.4 Effect of the bandwidth on the 1/rev response

One last study was made to analyze how a parameter change impacts on the 1/rev response vector obtained in chapter 4. In particular, it was observed the effect of the filter bandwidth variation, which appeared, during the developing stage, to be the most impactful among the input parameters.
First thing to note is that with a too wide of a pass band the response obtained starts to include unwanted harmonics, resulting in portions of the response with an higher frequency and therefore more periods than the ones in the keyphasor signal. When this happens, the phase calculation cannot be performed accurately, so an error is displayed to suggest the user to change parameters.

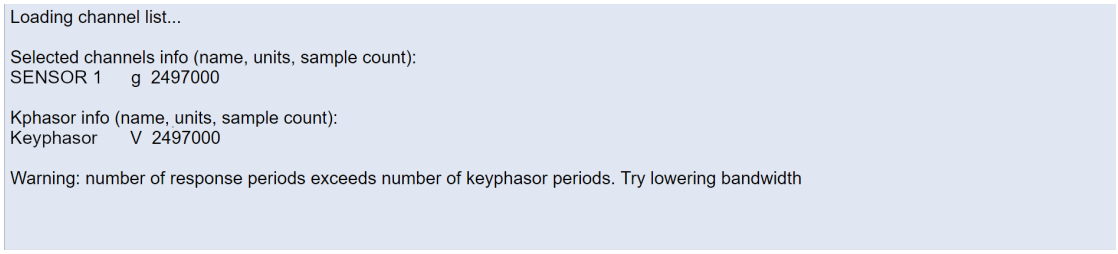

Figure 6.11: Error message displayed in case of 1/rev with wrong frequency

During the study, different bandwidth values have been considered, in the range between 7% and 21% of rotor frequency. Bandwidth above that range resulted in the aforementioned error. This limit is an empirical value that changes from a run to another depending on the composition of the raw signal, and can also change between two different sensor in the same run.

Figure 6.12 shows the various 1/rev responses obtained using different filter bandwidths in the considered range, given in terms of amplitude and phase. There can be seen that an higher bandwidth results in a growing amplitude and a slightly growing phase. The change in amplitude is due to the use of RMS to find the average value. The results, however, are still quite similar so that the variation does not really impact on the final balancing solution.

The three responses at higher bandwidth, the points on the right of the plot, present an abnormally higher phase than the previous one. This is a consequence of some unwanted noise which, while it is not caused by the chosen bandwidth per se, can be remove by reducing the pass band, as seen in the study.
The effect of the noise can be seen in figure 6.13. It causes a variation in the 1/rev frequency in one point, introducing an error in the phase measurement that propagates to all the subsequent periods.

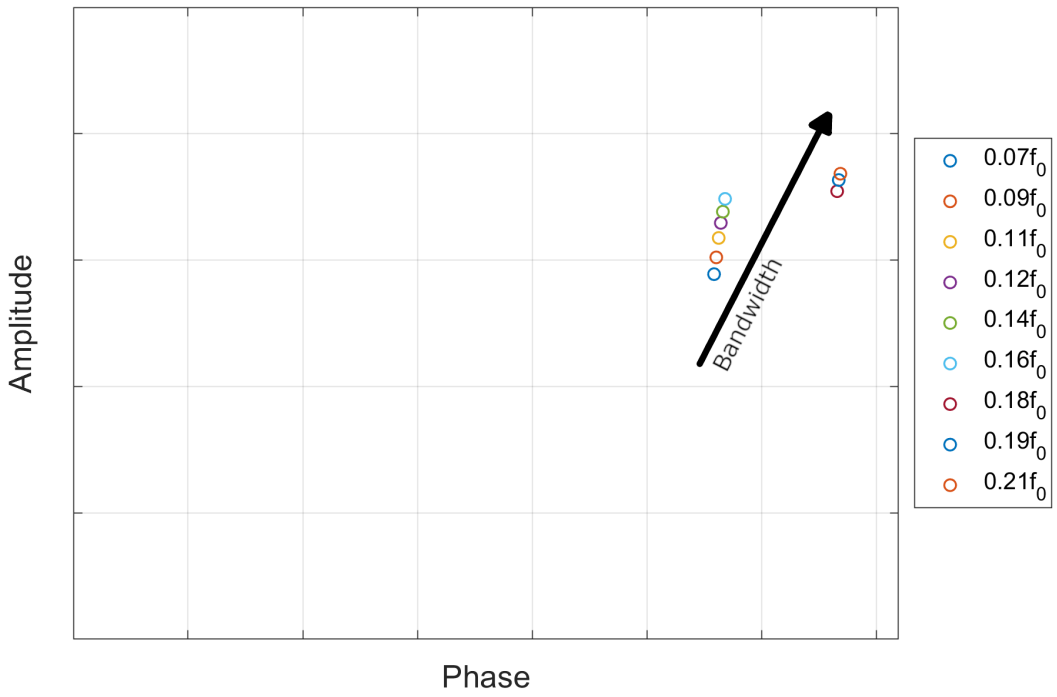

Figure 6.12: 1/rev responses obtained with different filter bandwidths

The cause of the noise can be better visualized by looking at the response signal in the frequency domain through an FFT (Fast Fourier Transform) analysis. In figure 6.14 is shown the FFT of the response taken in a point of the signal in which the noise is not significant. There can be seen that in the frequency range that passes through the filter there is one main response contribution that is the 1/rev component.
Figure 6.15 shows the response in the frequency domain analyzed where the detected noise has a significant impact. This time there can be seen how the contribution of the 1/rev response is not predominant on the other components that fall in the considered frequency range, which results in an impact of the noise on the response that is not negligible.

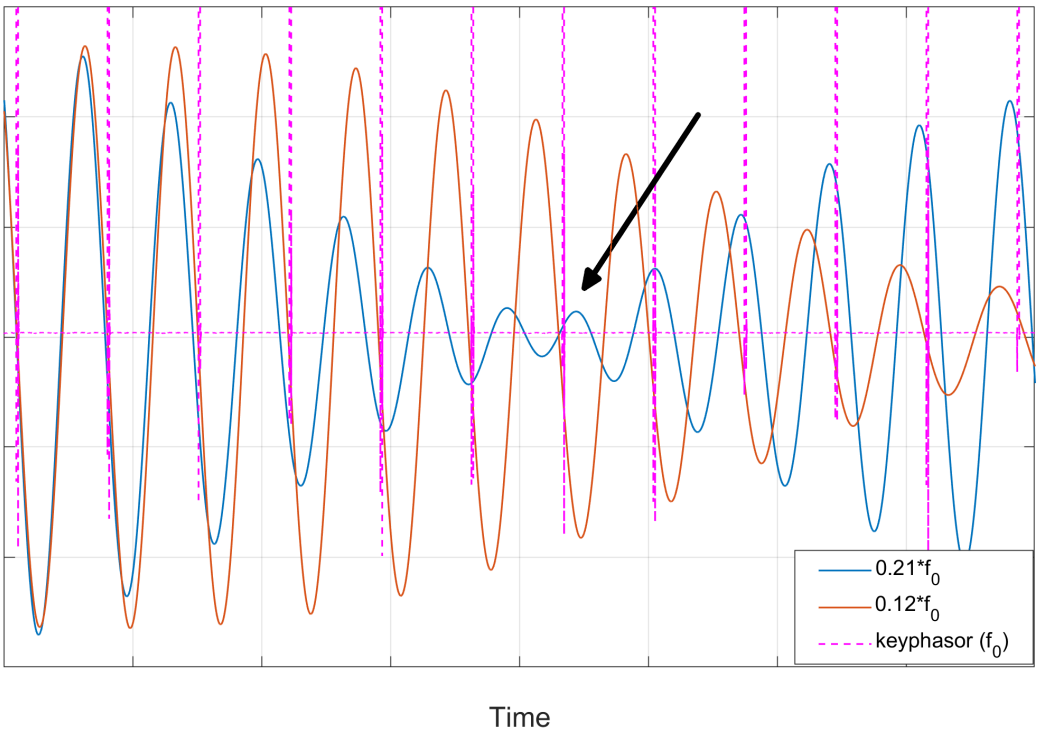

Figure 6.13: 1/rev response signal with and without noise

The influence of the noise that compromises the accuracy of the response vector calculated is, as already said, a particular case of the practical test, which cannot really be predicted. The physical cause, in this case, could probably be found in the fact that the rotor considered is a propeller. The blades of the propeller have a variable pitch, that is constantly adjusted by the system in order to maintain a constant speed. This continuous adjustments affect the 1/rev, causing an higher variation than the one expected and possibly introducing the disturbing noise.

Since it is difficult to accurately predict the presence of noise on the 1/rev, there is not a absolute way to define the best filter bandwidth to process the data. The ideal pass band can then be found with some experience and

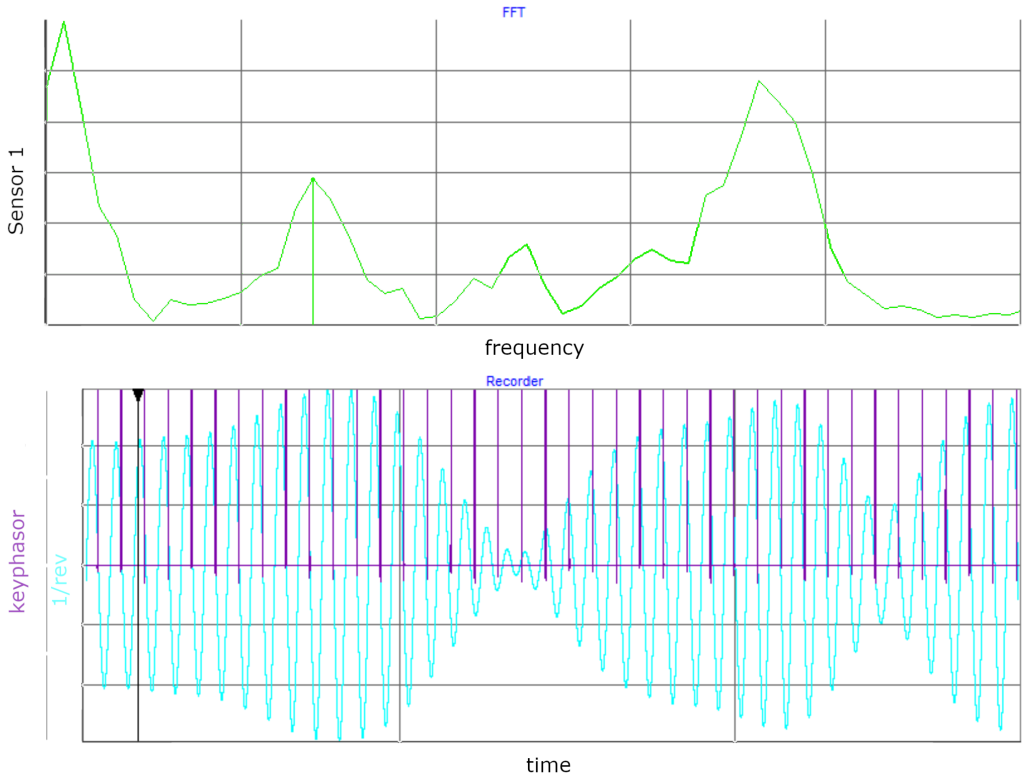

Figure 6.14: Frequency domain response in a point without noise on the 1/rev

eventually through a trial and error process, using the response output plots seen in chapter 4 to make sure that an error like the one here observed does not appear.

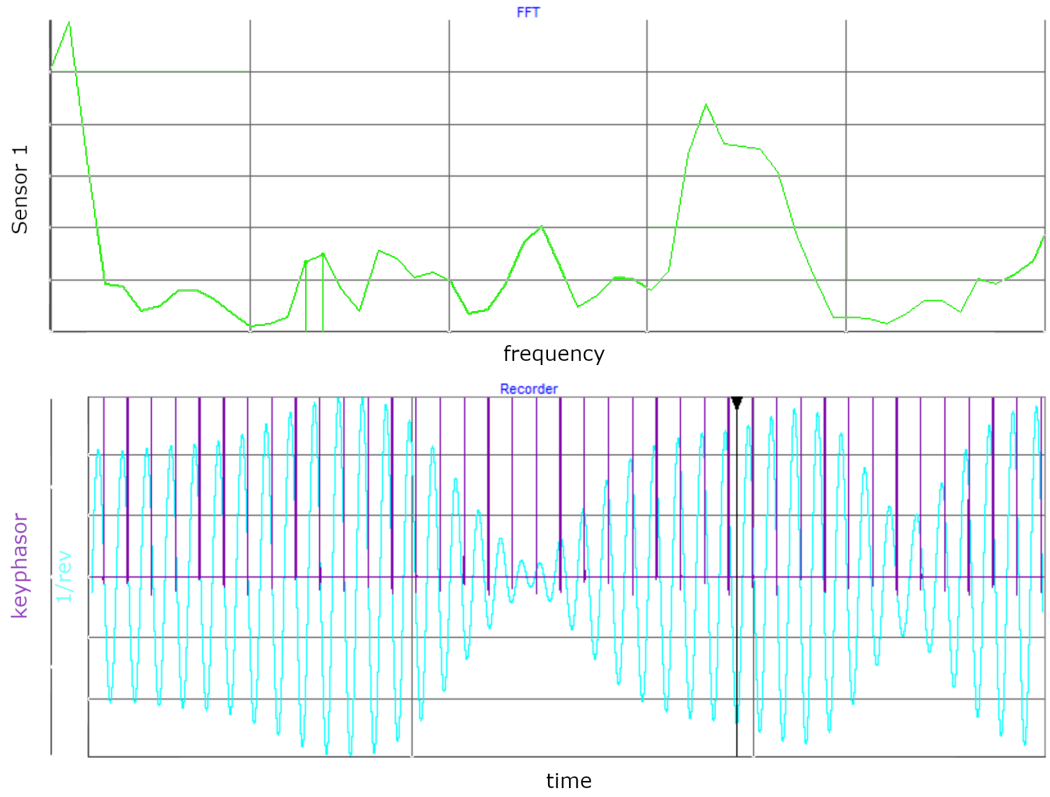

Figure 6.15: Frequency domain response in a point with noise on the 1/rev

Chapter 7

Conclusion

The objective of the work here presented was to develop a tool that would be able to read raw test data, process them and find a balance solution for the rotor. The tool has been designed to work with both analytical data, obtained from a modelized rotor, and actual raw test data. It has been validated using both kinds of data, with two tests for analytical data and one using test data.

The two analytical tests performed using a 2D model of a simple rotor show that the tool is extremely useful to reduce the system response by balancing out the rotors. The first analysis allowed to see that, in case of a rotor with an high modal response at lower frequencies, is possible to perform the balancing using data obtained by running the rotor at speeds lower than the critical speed, thus preventing possible dangerous events during the testing phase. When acting on modes at higher frequencies, however, using response data taken at speeds that are too low is much less effective.

Another thing that can be gathered by the analytical tests is that acting

on a mode at low frequency to reduce its response results in an increase of response at higher frequencies. Conversely, reducing the response at high frequencies causes an amplification on the modes at lower frequency. This means that a modal response cannot be fully removed, but only moved to different frequencies. This is the reason why we talk about modal placement. When balancing a rotor, then, there is not a perfect solution but only a compromise between the possible solutions. The best balance solution is the one whose side effects are not dangerous for the normal operation of the system and that possibly allows the lowest energy leaks caused by the vibrations.

The last test allows to check how the tool behaves when reading raw test data. Despite not having a balanced test run to which compare the solution with, the similarities between the solutions given by the three different combinations studied suggest that the tool is accurate. The balance solutions have also been verified using the previously available tool on which it was based, giving the same results and further confirming that the developed tool is able to accurately reproduce the balancing process of its predecessor.

At the end of the validations, the tool proved to be able to autonomously analyze the given test data with minimum help from the user. It is able to automatically generate the sensitivity coefficients, for both single and double balancing planes, and store them to be later used for future balancing of the same rotor family. The balancing can then be performed starting from data test both by finding new sensitivity factor, both by using already available coefficients.

Bibliography

[1] JC Austrow. «An optimum balance weight search algorithm». In: *ASME Journal article* (1994).

[2] T.P. Goodman. «Least squares formulation for multi-plane balancing». In: *ASME Journal article* ().

[3] Brice Carnahan, H. A. Luther, and James O. Wilkes. *Applied numerical methods*. Wiley, 1969. URL: https://cir.nii.ac.jp/crid/1130282269547088128.

[4] Giancarlo Genta. *Dynamics of rotating systems*. Springer Science & Business Media, 2005 (cit. on pp. 2, 4, 5, 8, 10).

[5] J.M. Vance, F.Y. Zeidan, and B.G. Murphy. *Machinery Vibration and Rotordynamics*. Wiley, 2010. ISBN: 9780470916070. URL: https://books.google.it/books?id=0zOIJIutYKQC (cit. on pp. 19, 20).

[6] J.M. Vance. *Rotordynamics of Turbomachinery*. A Wiley-Interscience Publication. Wiley, 1991. ISBN: 9780471802587. URL: https://books.google.it/books?id=8FLivi9MQcEC (cit. on p. 44).

[7] D. Childs. *Turbomachinery Rotordynamics: Phenomena, Modeling, and Analysis*. Wiley-Interscience publication. Wiley, 1993. ISBN: 9780471538400. URL: https://books.google.it/books?id=vKPfBxgQQPoC.

[8] A. Muszynska. *Rotordynamics*. Mechanical Engineering. CRC Press, 2005. ISBN: 9781420027792. URL: https://books.google.it/books?id=TEZuBwAAQBAJ (cit. on pp. 2, 24).

[9] Unknown. *What is filter order?* June 2023. URL: https://www.collimator.ai/reference-guides/what-is-filter-order (cit. on p. 31).

[10] Unknown. *Sinusoidi e fasori*. URL: https://www.edutecnica.it/elettrotecnica/fasori/fasori.htm (cit. on p. 7).

[11] Unknown. *EDV-DS-2221F-Lowres*. URL: https://buy.endevco.com/ContentStore/mktg/Downloads/EDV-DS-2221F_Lowres.pdf (cit. on p. 25).

[12] Ahmed Malim, Nikolaos Mourousias, Benoît Marinus, and Tim De Troyer. «UNSTEADY AEROELASTIC RESPONSE SIMULATION OF A 3D PRINTED HIGH ALTITUDE PROPELLER USING FLUID-STRUCTURE INTERACTION». In: June 2022 (cit. on p. 12).

[13] B. Daniele Zucca S. *Lecture slides of "Dinamica dei rotori per applicazioni aerospaziali"*. 2021 (cit. on p. 15).